arXiv:hep-ph/0103320v2 14 May 2001

SUSX-TH/01-016

EDM Constraints in Supersymmetric Theories

S. Abel[1,2], S. Khalil[1,3], and O. Lebedev[1]

[1]Centre for Theoretical Physics, University of Sussex, Brighton BN1 9QJ, U. K.

[2]IPPP, University of Durham, South Rd., Durham DH1 3LE , U. K.

[3]Ain Shams University, Faculty of Science, Cairo, 11566, Egypt.

Abstract

We systematically analyze constraints on supersymmetric theories imposed by the experimental bounds on the electron, neutron, and mercury electric dipole moments. We critically reappraise the known mechanisms to suppress the EDMs and conclude that only the scenarios with approximate CP-symmetry or flavour-off-diagonal CP violation remain attractive after the addition of the mercury EDM constraint.

1 Introduction

There are a number of reasons to suspect that there are additional sources of CP violation beyond those of the Standard Model (given by $\bar{\theta}$ and δ_{KM}). The most compelling one is that the SM is unable to explain the cosmological baryon asymmetry of our universe. Also, the Standard Model is very unlikely to be the "ultimate" theory of nature. Most extensions of the SM bring in new sources of CP-violation. In particular, the most attractive one – the Minimal Supersymmetric Standard Model (MSSM) allows for new sources of CP violation in both supersymmetry-breaking and supersymmetry-conserving sectors, and there are no compelling arguments for them to be zero. In addition, the improving precision in the measurements of the CP-observables such as $A_{CP}(B \to \psi K_s)$ [1] may soon reveal deviations from the SM predictions.

The most stringent constraints on models with additional sources of CP violation come from continued efforts to measure the electric dipole moments (EDM) of the neutron [2], electron [3], and mercury atom [4]

$$\begin{aligned} d_n &< 6.3 \times 10^{-26} \text{ e cm } (90\% CL), \\ d_e &< 4.3 \times 10^{-27} \text{ e cm }, \\ d_{Hg} &< 2.1 \times 10^{-28} \text{ e cm }. \end{aligned} \tag{1}$$

With the expected improvements in experimental precision, the EDM is likely to be one of the most important tests for physics beyond the Standard Model for some time to come, and EDMs will remain a difficult hurdle for supersymmetric theories if they are to allow sufficient baryogenesis. Indeed it is remarkable that the SM contribution to the EDM of the neutron is of order 10^{-30} e cm, whereas the "generic" supersymmetric value is 10^{-22}e cm.

In this paper we analyze neutron, electron, and mercury EDMs in the context of R-parity conserving supersymmetric theories. In particular, we reconsider the known mechanisms to suppress EDMs in light of the recently reported bound on the mercury EDM [4]. These include SUSY models with small CP phases, models with heavy sfermions, the cancellation scenario, and models with flavour off-diagonal CP violation. We also study to what extent different scenarios rely on assumptions about the neutron structure, i.e. chiral quark model *vs* parton model.

The paper is organized as follows. In section 2 we present general formulae for the EDMs and discuss their model-dependence. In section 3 we define our supersymmetric framework and present all relevant supersymmetric contributions to the EDMs. In particular, we analyze the importance of the two-loop Barr-Zee and Weinberg type EDM contributions. Section 4 is devoted to the study of the EDM suppression mechanisms. First we consider in detail the "canonical" scenarios: suppression due to small CP phases or heavy sfermions. Second, in the context of the cancellation scenario, we analyze the possibility of the EDM cancellations in two classes of models: mSUGRA-like models with nontrivial gaugino phases and D-brane models. Finally, we discuss the EDM suppression in models with flavour-off-diagonal CP violation. In addition, we present new model-independent bounds on the sfermion mass insertions imposed by the electron, neutron, and mercury electric dipole moments. In section 5 we overview and discuss our results.

2 Electron, neutron, and mercury electric dipole moments

Let us first summarize the contributions to the three most significant EDMs, beginning with the most reliable, the electron EDM.

2.1 Electron EDM

The electron EDM is defined by the effective CP-violating interaction

$$\mathcal{L} = -\frac{i}{2} d_e \bar{e} \sigma_{\mu\nu} \gamma_5 e \, F^{\mu\nu} \, , \tag{2}$$

where $F^{\mu\nu}$ is the electromagnetic field strength. The experimental bound on the electron EDM is derived from the electric dipole moment of the thallium atom and is given by [3]

$$d_e < 4 \times 10^{-27} \text{e cm} \, . \tag{3}$$

In supersymmetric models, the electron EDM arises due to CP-violating 1-loop diagrams with the chargino and neutralino exchange:

$$d_e = d_e^{\chi^+} + d_e^{\chi^0} \ . \tag{4}$$

Since the EEDM calculation involves little uncertainty it allows to extract reliable bounds on the CP-violating SUSY phases.

2.2 Neutron EDM

The neutron EDM has contributions from a number of CP-violating operators involving quarks, gluons, and photons. The most important ones include the electric and chromoelectric dipole operators, and the Weinberg three-gluon operator:

$$\begin{aligned} \mathcal{L} = & - \frac{i}{2} d_q^E \bar{q} \sigma_{\mu\nu} \gamma_5 q \ F^{\mu\nu} - \frac{i}{2} d_q^C \bar{q} \sigma_{\mu\nu} \gamma_5 T^a q \ G^{a\mu\nu} \\ & - \frac{1}{6} d^G f_{abc} G_{a\mu\rho} G^{\rho}_{b\nu} G_{c\lambda\sigma} \epsilon^{\mu\nu\lambda\sigma} \ , \end{aligned} \tag{5}$$

where $G_{a\mu\nu}$ is the gluon field strength, T^a and f_{abc} are the SU(3) generators and group structure coefficients, respectively. Given these operators, it is however a nontrivial task to evaluate the neutron EDM since assumptions about the neutron internal structure are necessary. In what follows we will study two models, namely the quark chiral model and the quark parton model. Neither of these models is sufficiently reliable by itself [5], however a power of the combined analysis should provide an insight into implications of the bound on the neutron EDM and in particular comparing them gives some indication of the importance of these systematic errors in, for example, cancellations. A better justified approach to the neutron EDM based on the QCD sum rules has appeared in [8] and earlier work [9], [13]. We note that in any case the NEDM calculations involve uncertain hadronic parameters such as the quark masses and thus these calculations have a status of estimates. The major conclusions of the present work are independent of the specifics of the neutron model.

i. Chiral quark model. This is a nonrelativistic model which relates the neutron EDM to the EDMs of the valence quarks with the help of the SU(6) coefficients:

$$d_n = \frac{4}{3} d_d - \frac{1}{3} d_u \ . \tag{6}$$

The quark EDMs can be *estimated* via Naive Dimensional Analysis [6] as

$$d_q = \eta^E d_q^E + \eta^C \frac{e}{4\pi} d_q^C + \eta^G \frac{e\Lambda}{4\pi} d^G \ , \tag{7}$$

where the QCD correction factors are given by $\eta^E = 1.53$, $\eta^C \simeq \eta^G \simeq 3.4$, and $\Lambda \simeq 1.19 \ GeV$ is the chiral symmetry breaking scale. We use the numerical values for these coefficients as given in [7]. The parameters $\eta^{C,G}$ involve considerable uncertainties

steming from the fact that the strong coupling constant at low energies is unknown. Another weak side of the model is that it neglects the sea quark contributions which play an important role in the nucleon spin structure.

The supersymmetric contributions to the dipole moments of the individual quarks result from the 1-loop gluino, chargino, neutralino exchange diagrams

$$d_q^{E,C} = d_q^{\tilde{g}\ (E,C)} + d_q^{\chi^+\ (E,C)} + d_q^{\chi^0\ (E,C)} \ , \tag{8}$$

and from the 2-loop gluino-quark-squark diagrams which generate d^G.

ii. Parton quark model. This model is based on the isospin symmetry and known contributions of different quarks to the spin of the proton [10]. The quantities Δ_q defined as $\langle n|\frac{1}{2}\bar{q}\gamma_\mu\gamma_5 q|n\rangle = \Delta_q\ S_\mu$, where S_μ is the neutron spin, are related by the isospin symmetry to the quantities $(\Delta_q)_p$ which are measured in the deep inelastic scattering (and other) experiments, i.e. $\Delta_u = (\Delta_d)_p$, $\Delta_d = (\Delta_u)_p$, and $\Delta_s = (\Delta_s)_p$. To be exact, the neutron EDM depends on the (yet unknown) tensor charges rather than these axial charges. The main *assumption* of the model is that the quark contributions to the NEDM are weighted by the same factors Δ_i, i.e. [10]

$$d_n = \eta^E(\Delta_d d_d^E + \Delta_u d_u^E + \Delta_s d_s^E) \ . \tag{9}$$

In our numerical analysis we use the following values for these quantities $\Delta_d = 0.746$, $\Delta_u = -0.508$, and $\Delta_s = -0.226$ as they appear in the analysis of Ref.[11]. As before, we have

$$d_q^E = d_q^{\tilde{g}\ (E)} + d_q^{\chi^+\ (E)} + d_q^{\chi^0\ (E)} \ . \tag{10}$$

The major difference from the chiral quark model is a large strange quark contribution (which is likely to be an overestimate [5]). In particular, due to the large strange and charm quark masses, the strange quark contribution dominates in most regions of the parameter space. This leads to considerable numerical differences between the predictions of the two models.

The current experimental limit on the neutron EDM is [2]

$$d_n < 6.3 \times 10^{-26}\text{e cm} \ . \tag{11}$$

2.3 Mercury EDM

The EDM of the mercury atom results mostly from T-odd nuclear forces in the mercury nucleus [12], which induce the effective interaction of the type $(\mathbf{I}\cdot\nabla)\delta(\mathbf{r})$ between the electron and the nucleus of spin $\mathbf{I}$ [5]. In turn, the T-odd nuclear forces arise due to the effective 4-fermion interaction $\bar{p}p\bar{n}i\gamma_5 n$. It has been argued [5] that the mercury EDM is primarily sensitive to the chromoelectric dipole moments of the quarks and the limit [4]

$$d_{Hg} < 2.1 \times 10^{-28}\text{e cm} \tag{12}$$

can be translated into

$$|d_d^C - d_u^C - 0.012 d_s^C|/g_s < 7 \times 10^{-27}\text{cm} \ , \tag{13}$$

where g_s is the strong coupling constant. As in the parton neutron model, there is a considerable strange quark contribution. The relative coefficients of the quark contributions in (13) are known better than those for the neutron, however the overall normalization is still not free of uncertainties [13].

3 The EDMs in SUSY models

We will study supersymmetric models with the following high energy scale soft breaking potential

$$\begin{aligned} V_{SB} &= m_{0\alpha}^2 \phi_\alpha^* \phi_\alpha - (B\mu H_1 H_2 + h.c.) + (A_l Y_{ij}^l \; H_1 \tilde{l}_{Li} \tilde{e}_{Rj}^* + A_d Y_{ij}^d \; H_1 \tilde{q}_{Li} \tilde{d}_{Rj}^* \\ &- A_u Y_{ij}^u \; H_2 \tilde{q}_{Li} \tilde{u}_{Rj}^* + h.c.) + \frac{1}{2}(m_3 \overline{\tilde{g}} \tilde{g} + m_2 \overline{\tilde{W}^a} \tilde{W}^a + m_1 \overline{\tilde{B}} \tilde{B}) \; , \end{aligned} \tag{14}$$

where ϕ_α denotes all the scalars of the theory. We generally allow for $A_l \neq A_u \neq A_d$ as well as nonuniversal gaugino and scalar masses, which is important for the analysis of D-brane models. The μ, B, A_α, and m_i parameters can be complex, however two of their phases can be eliminated by the $U(1)_R$ and $U(1)_{PQ}$ transformations under which these parameters behave as spurions. The Peccei-Quinn transformation acts on the Higgs doublets and the "right-handed" superfields in such a way that all the interactions but those which mix the two doublets are invariant. The Peccei-Quinn charges are $Q_{PQ}(\mu) = Q_{PQ}(B\mu)$, $Q_{PQ}(A) = Q_{PQ}(m_i) = 0$. The $U(1)_R$ transforms the Grassmann variable $\theta \to \theta e^{i\alpha}$ and the fields in such a way that the integral of the superpotential over the Grassmann variables is invariant, i.e. the $U(1)_R$ charge of the superpotential is 2. As a result, $Q_R(B\mu) = Q_R(\mu) - 2$, $Q_R(A) = Q_R(m_i) = -2$. The six physical CP-phases of the theory are invariant under both $U(1)_R$ and $U(1)_{PQ}$, and can be chosen as

$$Arg(A_d^* m_i) \; , \; Arg((B\mu)^* \mu A_\alpha) \; , \tag{15}$$

where $i = 1, 2, 3$ and $\alpha = d, u, l$. All other CP-phases can be expressed as their linear combinations. If the A-terms are universal, there are four physical phases $Arg(A^* m_i)$, $Arg((B\mu)^* \mu A)$.

It is customary to choose the phase convention in which the Higgs potential parameter $B\mu$ is real. In this case, the physical phases become $Arg(A_d^* m_i)$ and $Arg(\mu A_\alpha)$. If universality is assumed, the number of physical phases reduces to two. In what follows we will set m_2 to be real by a $U(1)_R$ rotation.

Nonuniversality will play a crucial role in the D-brane and flavour models' analysis, but otherwise does not lead to different conclusions for the models we study. Thus we will assume universal A-terms and gaugino masses unless otherwise specified.

In what follows we use $\tan\beta$, m_0, A, m_i as input parameters and obtain low energy quantities via the MSSM renormalization group equations (RGE). We also assume radiative electroweak symmetry breaking, i.e. that the magnitude of the μ parameter is given (at tree level) by

$$|\mu|^2 = \frac{m_{H_1}^2 - m_{H_2}^2 \tan^2\beta}{\tan^2\beta - 1} - \frac{1}{2} m_Z^2 \; . \tag{16}$$

The phase of μ is an input parameter and is RG-invariant. Our numerical results are sensitive to the quark masses which we fix at the M_Z scale to be: $m_{u_i} = (0.005, 1.40, 165)$ GeV and $m_{d_i} = (0.010, 0.194, 3.54)$ GeV. The light quark masses are poorly determined (in fact $m_u = 0$ is not excluded) which results in the uncertainties of the EDM normalization; for definiteness, we have chosen the light quark masses as they appear in [7]. The GUT scale is assumed to be 2×10^{16} GeV.

It is well known that $\mathcal{O}(1)$ supersymmetric CP phases generally lead to unacceptably large electric dipole moments which constitutes the SUSY CP problem. In this paper we consider different mechanisms for suppressing EDMs and analyze them in detail.

3.1 Leading SUSY contributions to the EDMs

In this subsection we list formulae for individual supersymmetric contributions to the EDMs due to the Feynman diagrams in Fig.1. In our presentation we follow the work of Ibrahim and Nath [7].

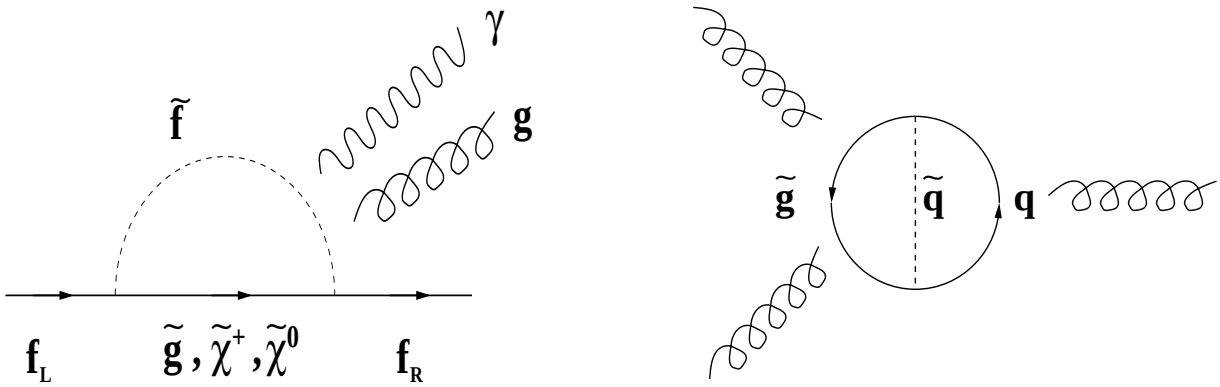


Figure 1: Leading SUSY contributions to the EDMs. The photon and gluon lines are to be attached to the loop in all possible ways.

Neglecting the flavour mixing, the electromagnetic contributions to the fermion EDMs are given by [7]:

$$d_q^{\tilde{g}\,(E)}/e = \frac{-2\alpha_s}{3\pi}\sum_{k=1}^{2}\mathrm{Im}(\Gamma_q^{1k})\frac{m_{\tilde{g}}}{M^2_{\tilde{q}_k}}Q_{\tilde{q}}\,\mathrm{B}\Big(\frac{m^2_{\tilde{g}}}{M^2_{\tilde{q}_k}}\Big)\,,$$

$$d_u^{\chi^+\,(E)}/e = \frac{-\alpha_{em}}{4\pi\sin^2\theta_W}\sum_{k=1}^{2}\sum_{i=1}^{2}\mathrm{Im}(\Gamma_{uik})\frac{m_{\chi_i^+}}{M^2_{\tilde{d}_k}}\Big[Q_{\tilde{d}}\,\mathrm{B}\Big(\frac{m^2_{\chi_i^+}}{M^2_{\tilde{d}_k}}\Big)+(Q_u-Q_{\tilde{d}})\,\mathrm{A}\Big(\frac{m^2_{\chi_i^+}}{M^2_{\tilde{d}_k}}\Big)\Big]\,,$$

$$d_d^{\chi^+\,(E)}/e = \frac{-\alpha_{em}}{4\pi\sin^2\theta_W}\sum_{k=1}^{2}\sum_{i=1}^{2}\mathrm{Im}(\Gamma_{dik})\frac{m_{\chi_i^+}}{M^2_{\tilde{u}_k}}\Big[Q_{\tilde{u}}\,\mathrm{B}\Big(\frac{m^2_{\chi_i^+}}{M^2_{\tilde{u}_k}}\Big)+(Q_d-Q_{\tilde{u}})\,\mathrm{A}\Big(\frac{m^2_{\chi_i^+}}{M^2_{\tilde{u}_k}}\Big)\Big]\,,$$

$$d_e^{\chi^+}/e = \frac{\alpha_{em}}{4\pi\sin^2\theta_W}\sum_{i=1}^{2}\frac{m_{\chi_i^+}}{m^2_{\tilde{\nu}}}\mathrm{Im}(\Gamma_{ei})\,\mathrm{A}\Big(\frac{m^2_{\chi_i^+}}{m^2_{\tilde{\nu}}}\Big)\,,$$

$$d_f^{\chi^0\,(E)}/e = \frac{\alpha_{em}}{4\pi\sin^2\theta_W}\sum_{k=1}^{2}\sum_{i=1}^{4}\mathrm{Im}(\eta_{fik})\frac{m_{\chi_i^0}}{M^2_{\tilde{f}_k}}Q_{\tilde{f}}\,\mathrm{B}\Big(\frac{m^2_{\chi_i^0}}{M^2_{\tilde{f}_k}}\Big)\,. \tag{17}$$

Here

$$\Gamma_q^{1k} = e^{-i\phi_3}D_{q2k}D^*_{q1k}\,, \tag{18}$$

with ϕ_3 being the gluino phase and D_q defined by $D_q^\dagger M^2_{\tilde{q}} D_q = \mathrm{diag}(M^2_{\tilde{q}_1}, M^2_{\tilde{q}_2})$. The sfermion mass matrix $M^2_{\tilde{f}}$ is given by

$$M^2_{\tilde{f}} = \begin{pmatrix} {M_L}^2 + {m_f}^2 + M_z^2(\frac{1}{2} - Q_f\sin^2\theta_W)\cos 2\beta & m_f(A_f^* - \mu R_f) \\ m_f(A_f - \mu^* R_f) & M_R^2 + {m_f}^2 + M_z^2 Q_f \sin^2\theta_W\ \cos 2\beta \end{pmatrix}\,,$$

where $R_f = \cot\beta$ ($\tan\beta$) for $I_3 = 1/2$ ($-1/2$). The chargino vertex Γ_{fik} is defined as

$$\begin{aligned}\Gamma_{uik} &= \kappa_u V^*_{i2} D_{d1k}(U^*_{i1}D^*_{d1k} - \kappa_d U^*_{i2}D^*_{d2k})\,,\\ \Gamma_{dik} &= \kappa_d U^*_{i2} D_{u1k}(V^*_{i1}D^*_{u1k} - \kappa_u V^*_{i2}D^*_{u2k})\end{aligned} \tag{19}$$

and analogously for the electron; here U and V are the unitary matrices diagonalizing the chargino mass matrix: $U^* M_{\chi^+} V^{-1} = \mathrm{diag}(m_{\chi_1^+}, m_{\chi_2^+})$. The quantities κ_f are the Yukawa couplings

$$\kappa_u = \frac{m_u}{\sqrt{2}m_W\sin\beta},\quad \kappa_{d,e} = \frac{m_{d,e}}{\sqrt{2}m_W\cos\beta}. \tag{20}$$

The neutralino vertex η_{fik} is given by

$$\begin{aligned}\eta_{fik} &= \Big[-\sqrt{2}\{\tan\theta_W(Q_f - I_{3_f})X_{1i} + I_{3_f}X_{2i}\}D^*_{f1k} - \kappa_f X_{bi}D^*_{f2k}\Big]\\ &\times \Big[\sqrt{2}\tan\theta_W Q_f X_{1i}D_{f2k} - \kappa_f X_{bi}D_{f1k}\Big]\,,\end{aligned} \tag{21}$$

where I_3 is the third component of the isospin, $b = 3$ (4) for $I_3 = -1/2$ (1/2), and X is the unitary matrix diagonalizing the neutralino mass matrix: $X^T M_{\chi^0} X = \mathrm{diag}(m_{\chi_1^0}, m_{\chi_2^0}, m_{\chi_3^0}, m_{\chi_4^0})$. In our convention the mass matrix eigenvalues are positive and ordered as $m_{\chi_1^0} > m_{\chi_2^0} > ...$ (this holds for all mass matrices in the paper). The loop functions $A(r), B(r)$, and $C(r)$ are defined by

$$\begin{aligned}A(r) &= \frac{1}{2(1-r)^2}\Big(3 - r + \frac{2\ln r}{1-r}\Big)\,,\\ B(r) &= \frac{1}{2(r-1)^2}\Big(1 + r + \frac{2r\ln r}{1-r}\Big)\,,\\ C(r) &= \frac{1}{6(r-1)^2}\Big(10r - 26 + \frac{2r\ln r}{1-r} - \frac{18\ln r}{1-r}\Big)\,.\end{aligned} \tag{22}$$

The chromoelectric contributions to the quark EDMs are given by

$$\begin{aligned}d_q^{\tilde{g}\,(C)} &= \frac{g_s\alpha_s}{4\pi}\sum_{k=1}^{2}\mathrm{Im}(\Gamma_q^{1k})\frac{m_{\tilde{g}}}{M^2_{\tilde{q}_k}}\,\mathrm{C}\Big(\frac{m^2_{\tilde{g}}}{M^2_{\tilde{q}_k}}\Big)\,,\\ d_q^{\chi^+\,(C)} &= \frac{-g^2 g_s}{16\pi^2}\sum_{k=1}^{2}\sum_{i=1}^{2}\mathrm{Im}(\Gamma_{qik})\frac{m_{\chi_i^+}}{M^2_{\tilde{q}_k}}\,\mathrm{B}\Big(\frac{m^2_{\chi_i^+}}{M^2_{\tilde{q}_k}}\Big)\,,\\ d_q^{\chi^0\,(C)} &= \frac{g_s g^2}{16\pi^2}\sum_{k=1}^{2}\sum_{i=1}^{4}\mathrm{Im}(\eta_{qik})\frac{m_{\chi_i^0}}{M^2_{\tilde{q}_k}}\,\mathrm{B}\Big(\frac{m^2_{\chi_i^0}}{M^2_{\tilde{q}_k}}\Big)\,.\end{aligned} \tag{23}$$

Finally, the contribution to the Weinberg operator [14] from the two-loop gluino-top-stop and gluino-bottom-sbottom diagrams reads

$$d^G = -3\alpha_s m_t \Big(\frac{g_s}{4\pi}\Big)^3 \,\mathrm{Im}(\Gamma_t^{12})\,\frac{z_1 - z_2}{m_{\tilde{g}}^3}\,\mathrm{H}(z_1, z_2, z_t) + \ (t \to b)\ , \tag{24}$$

where $z_i = \left(\frac{M_{\tilde{t}_i}}{m_{\tilde{g}}}\right)^2, z_t = \left(\frac{m_t}{m_{\tilde{g}}}\right)^2$. The two-loop function $H(z_1, z_2, z_t)$ is given by [15]

$$H(z_1, z_2, z_t) = \frac{1}{2}\int_0^1 dx \int_0^1 du \int_0^1 dy\; x(1-x)u\frac{N_1 N_2}{D^4}\ , \tag{25}$$

where

$$\begin{aligned} N_1 &= u(1-x) + z_t x(1-x)(1-u) - 2ux[z_1 y + z_2(1-y)]\ , \\ N_2 &= (1-x)^2(1-u)^2 + u^2 - \frac{1}{9}x^2(1-u)^2\ , \\ D &= u(1-x) + z_t x(1-x)(1-u) + ux[z_1 y + z_2(1-y)]\ . \end{aligned} \tag{26}$$

The numerical behaviour of this function was studied in [15]. We emphasize that the b-quark contribution is significant and often exceeds the top one.

Before we proceed to the discussion of the EDM suppression mechanisms, let us consider the effect of other potentially nonnegligible two-loop contributions.

3.2 Barr-Zee type EDM contributions

In view of considerable recent interest in the subject we will consider the two-loop Barr-Zee type contributions separately. We will follow the work of Chang, Keung, and Pilaftsis [16].

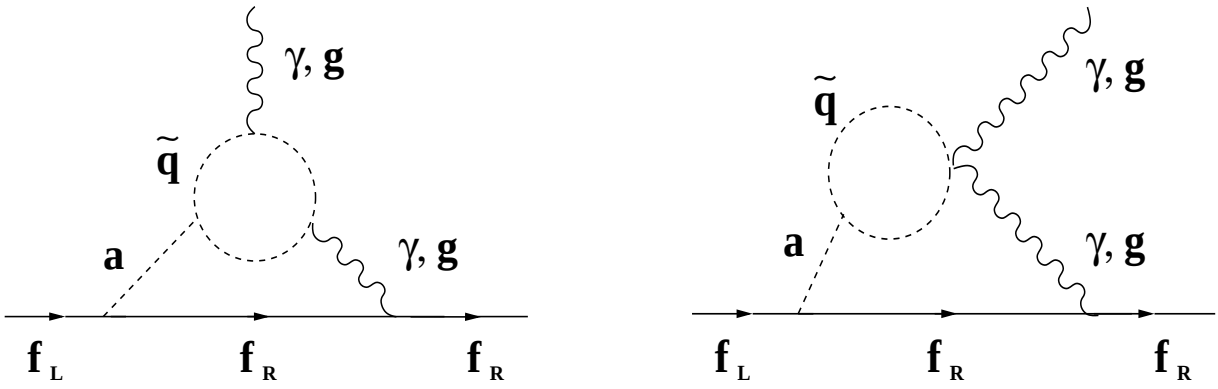


Figure 2: Barr-Zee type contributions to the EDMs.

In Ref.[17] Barr and Zee have presented two-loop Higgs-mediated EDM contributions which can be competetive with the Weinberg three-gluon operator. A supersymmetric version of the Barr-Zee graphs (Fig.2) was studied in [16]. In what follows we

will analyze only the leading contributions to the EDMs presented in [16]. The EDMs arise due to CP-violating couplings of the (s)fermions to the CP-odd Higgs boson a_0. The EDM and the CEDM of a light fermion f are computed to be [16]

$$d_f^E/e = Q_f \, \frac{3\alpha_{em}}{32\pi^3} \, \frac{R_f m_f}{M_a^2} \sum_{q=t,b} \xi_q Q_q^2 \Big[F\Big(\frac{M_{\tilde{q}_1}^2}{M_a^2}\Big) - F\Big(\frac{M_{\tilde{q}_2}^2}{M_a^2}\Big) \Big] \, ,$$
$$d_f^C = \frac{g_s \alpha_s}{64\pi^3} \, \frac{R_f m_f}{M_a^2} \sum_{q=t,b} \xi_q \Big[F\Big(\frac{M_{\tilde{q}_1}^2}{M_a^2}\Big) - F\Big(\frac{M_{\tilde{q}_2}^2}{M_a^2}\Big) \Big] \, , \qquad (27)$$

where $R_f = \cot\beta$ ($\tan\beta$) for $I_3 = 1/2$ ($-1/2$) and the two-loop function $F(z)$ is

$$F(z) = \int_0^1 dx \frac{x(1-x)}{z - x(1-x)} \ln\Big[\frac{x(1-x)}{z}\Big] \, . \qquad (28)$$

The CP-violating couplings $\xi_{t,b}$ are given by

$$\xi_t = -\frac{\sin 2\theta_{\tilde{t}} m_t \mathrm{Im}(\mu e^{i\delta_t})}{2v^2 \sin^2\beta} \, ,$$
$$\xi_b = \frac{\sin 2\theta_{\tilde{b}} m_b \mathrm{Im}(A_b e^{-i\delta_b})}{2v^2 \sin\beta\cos\beta} \, , \qquad (29)$$

with $\theta_{\tilde{t},\tilde{b}}$ being the standard stop and sbottom mixing angles; $\delta_q = \mathrm{Arg}(A_q - R_q \mu^*)$ and v=174 GeV. Note the difference from [16] in the definitions of μ and v, also see the corresponding Erratum.

In our numerical analysis, besides assuming the radiative electroweak symmetry breaking, we use the following tree level mass of the CP-odd Higgs [18]

$$M_a^2 = m_{H_1}^2 + m_{H_2}^2 + 2|\mu|^2 \, , \qquad (30)$$

which is a function of $\tan\beta$ and other GUT scale input parameters. Strictly speaking, this formula is valid for a CP-conserving case, however the EDMs are not very sensitive to the exact value of M_a^2 and an inclusion of loop corrections and CP-phases does not alter our results.

In Fig.4 we present a typical Barr-Zee type EDM behaviour as a function of $\tan\beta$ for $\phi_A = \pi/2$, $\phi_\mu = 0$. The other parameters are fixed to be $m_0 = m_{1/2} = A = 200$ GeV. The values of $\tan\beta$ beyond 42 are not displayed for this parameter set since the CP-odd scalar becomes massless in this region and the pattern of the EW symmetry breaking becomes unacceptable. We observe that generally these EDM contributions by themselves do not impose significant constraints on the GUT scale A-term phases even at large $\tan\beta$; as can be seen from the plot, the Barr-Zee contributions typically are one-two orders of magnitude below the experimental limit. One of the reasons for this is that the third generation A-term phases reduce by an order of magnitude due to the RG evolution at large $\tan\beta$. Also the value of the μ parameter is typically below 500 GeV owing to the radiative electroweak symmetry breaking. Other factors which distinguish our results from those of [16] are the imposition of Eq.(30) and utilization of

the chiral quark neutron model[1]. For comparison, in Fig.4 we provide the contribution of the Weinberg operator which also arises at the two-loop level.

The constraints become more restrictive for larger A-terms ($\sim 3m_0$) and larger m_0/m_3 ratios. In Fig.5 we set $m_0 = 500$ GeV, $m_{1/2} = 200$ GeV, and $A = 600$ GeV. In this case the A-term phase is not "diluted" as much as before and for some parameters the Barr-Zee EDMs can be close to the experimental limit. A similar effect can be achieved in models with non-universal gaugino masses by introducing a $\mathcal{O}(1)$ gluino phase. With the parameter set of Fig.5 the CP-odd Higgs becomes unacceptably light around $\tan\beta \simeq 36$.

¿From the point of view of low energy theory, the Barr-Zee type contributions can provide useful constraints on the phases of the third generation A-terms [16],[19]. One can imagine a situation in which the first two generation CP-violating effects are suppressed (as in the decoupling scenario), then the EDMs would constrain the third generation phases. We find however that typically the Weinberg three-gluon operator is considerably more sensitive to such phases and provides more severe constraints even at large $\tan\beta$[2]. For example, for the parameters of Figs.4 and 5 the contribution of the Weinberg operator exceeds that of the Barr-Zee type graphs by one-two orders of magnitude.

Finally, the Z- and W-mediated Barr-Zee type graphs have been analyzed in [20] and found to be significantly smaller than those considered above. A number of other subleading two loop contributions such as the gluino CEDM-induced quark EDMs, etc. have been studied in [21].

Although taken into account, this entire class of diagrams is numerically unimportant in our analysis.

4 Suppression of the EDMs in SUSY models

4.1 Small CP-phases

For a light (below 1 TeV) supersymmetric spectrum, the SUSY CP phases have to be small in order to satisfy the experimental EDM bounds (unless EDM cancellations occur). In Figs.6-8 we illustrate the EDMs behaviour as a function of the CP-phases in the mSUGRA-type models, where we have set $m_0 = m_{1/2} = A = 200$ GeV. At low $\tan\beta$, the EDM constraints impose the following bounds (at the GUT scale):

$$\begin{aligned} &\phi_A \leq 10^{-2} - 10^{-1} \,, \\ &\phi_\mu \leq 10^{-3} - 10^{-2} \,, \\ &\phi_{gaug.} \leq 10^{-2} \,. \end{aligned} \tag{31}$$

For $\tan\beta > 3$, these bounds become even stricter (for ϕ_μ and $\phi_{gaug.}$ the bounds are roughly inversely proportional to $\tan\beta$). We note that ϕ_A is less constrained than ϕ_μ

[1] We observe similar behaviour in the parton quark model.

[2] The Weinberg operator contribution can be suppressed by increasing the gluino mass. However, in mSUGRA the Barr-Zee type contributions will also get a suppression factor due to the RG "dilution" of the phases of the third generation A-terms.

and $\phi_{gaug.}$. There are two reasons for that: first, ϕ_A is reduced by the RG running from the GUT scale down to the electroweak scale and, second, the phase of the $(\delta^d_{11})_{LR}$ mass insertion which gives the dominant contribution to the EDMs is more sensitive to ϕ_μ and $\phi_{gaug.}$ due to $|A| < \mu \tan\beta$.

SUSY models with small CP-phases can be motivated by the approximate CP symmetry [22]. The well established experimental results exhibit small degree of CP violation. Thus it is conceivable that all existing CP-phases are small, including the CKM phase. The smallness of CP violation can be explained, for example, by a small ratio of the scale at which the CP symmetry gets broken spontaneously and the scale at which it is communicated to the observable sector.

Currently the CKM phase is consistent with zero and it could be supersymmetry that is responsible for the observed values of ε and ε'. This does not require large supersymmetric phases. In fact in models with non-universal A-terms ε and ε' can even be saturated with $\mathcal{O}(10^{-2})$ phase of the mass insertion $(\delta^d_{12})_{LR}$ [23]. In this case, $|(\delta^d_{12})_{LR}|$ is required to be $\mathcal{O}(10^{-3})$ which naturally appears in models with matrix-factorizable A-terms of the form $B \cdot Y_\alpha \cdot C$, where B and C are flavour matrices. The EDM bounds serve to constrain the flavour structure of B and C. Another possibility to produce the desired $(\delta^d_{12})_{LR}$ is to use asymmetric A-term textures in string-motivated models (where the standard supergravity relation $\hat{A}_{ij} = A_{ij} Y_{ij}$ is assumed).

Encouragingly, the phase of the μ-term of order 10^{-2} may be sufficient to produce the observed baryon asymmetry [24], which is in marginal agreement with the EDM bounds. The hypothesis of the approximate CP symmetry is currently being tested in the B physics experiments where the Standard Model predicts large CP-asymmetries. It is noteworthy that the smallness of the CP-phases in this picture does not constitute fine-tuning according to the t'Hooft's criterion [25] since setting them to zero would increase the symmetry of the theory.

We remark that small CP-phases may also arise due to the dynamics of the system. For instance, in weakly coupled heterotic string models, small soft and CKM phases arise when the T-moduli get VEV's close to the edge of the fundamental domain which is often the case [26]. This mechanism however relies on the assumption that the dilaton has a real VEV, so this model as it stands does not solve the SUSY CP problem. Nevertheless, it may serve as a step toward a consistent string model with naturally small CP phases.

Note that EDMs constrain only the *physical* phases (15). One can imagine a situation when the individual phases are $\mathcal{O}(1)$ whereas the physical ones are small. This occurs for example in gauge mediated SUSY breaking models, see [22] and references therein.

4.2 Heavy SUSY scalars

This possibility is based on the decoupling of heavy supersymmetric particles. Even if one allows $\mathcal{O}(1)$ CP violating phases, their effect will be negligible if the SUSY spectrum is sufficiently heavy [27]. Generally, SUSY fermions are required to be lighter than the SUSY scalars by, for example, cosmological considerations. So the decoupling scenario

can be implemented with heavy sfermions only. Here the SUSY contributions to the EDMs are suppressed even with maximal SUSY phases because the squarks in the loop are very heavy and the mixing angles are small.

In Fig.9 we display the EDMs as functions of the universal scalar mass parameter m_0 for the mSUGRA model with maximal CP-phases $\phi_\mu = \phi_A = \pi/2$ and $m_{1/2} = A = 200$ GeV. We observe that all EDM constraints except for that of the electron require m_0 to be around 5 TeV or more. The mercury constraint is the strongest one and requires

$$(m_0)_{decoupl.} \simeq 10 \text{ TeV} . \tag{32}$$

This leads to a serious fine-tuning problem. Recall that one of the primary motivations for supersymmetry was a solution to the naturalness problem. Certainly this motivation will be entirely lost if a SUSY model reintroduces the same problem in a different sector, i.e. for example a large hierarchy between the scalar mass and the electroweak scale.

The degree of fine-tuning can be quantified as follows. The Z boson mass is determined at tree level by

$$\frac{1}{2} m_Z^2 = \frac{m_{H_1}^2 - m_{H_2}^2 \tan^2\beta}{\tan^2\beta - 1} - \mu^2 . \tag{33}$$

One can define the sensitivity coefficients [28],[29]

$$c_i \equiv \left| \frac{\partial \ln m_Z^2}{\partial \ln a_i^2} \right| , \tag{34}$$

where a_i are the high energy scale input parameters such as $m_{1/2}$, m_0, etc. Note that μ is treated here as an independent input parameter. A value of c_i much greater than one would indicate a large degree of fine-tuning. The Higgs mass parameters are quite sensitive to m_0, so for m_0=10 TeV we find

$$c_{m_0} \sim 5000 \tag{35}$$

for the parameters of Fig.9. For the universal scalar mass of 5 (3) TeV the sensitivity coefficient reduces to 1300 (500). This clearly indicates an unacceptable degree of fine-tuning.

This problem can be mitigated in models with focus point supersymmetry, i.e. when m_{H_2} is insensitive to m_0 [29]. However, this mechanism works for m_0 no greater than 2-3 TeV which is not sufficient to suppress the EDMs. Another interesting possibility is presented by models with a radiatively driven inverted mass hierarchy, i.e. the models in which a large hierarchy between the Higgs and the first two generations scalar masses is created radiatively [30]. However, a successful implementation of this idea is far from trivial [31]. One can also break the scalar mass universality at the high energy scale [32]. In this case, either a mass hierarchy appears already in the soft breaking terms or certain relations among the soft parameters must be imposed (for a review see [33]). These significant complications disfavour the decoupling scenario as a way to solve the SUSY CP problem, yet it remains a possibility.

Note that the decoupling scenario rules out supersymmetry as a possible explanation of the recently observed 2.6 σ deviation in the muon $g-2$ from the SM prediction

[34]. This scenario may also lead to cosmological difficulties, in particular with the relic abundance of the LSPs since the LSP annihilation cross section falls rapidly as $m_{sfermion}$ increases. Concerning the other phenomenological consequences, we remark that the SUSY contributions to the CP-observables involving the first two generations (such as $\varepsilon, \varepsilon'$) are negligible, although those involving the third generation may be considerable. The corresponding CP-phases are constrained through the Weinberg operator contribution to the neutron EDM, which typically prohibits the maximal phase $\phi_{A_{t,b}}\Big|_{GUT} = \pi/2$ while still allowing for smaller $\mathcal{O}(1)$ phases (Fig.4).

4.3 EDM cancellations

The cancellation scenario is based on the fact that large cancellations among different contributions to the EDMs are possible in certain regions of the parameter space [7],[36],[37],[11] which allow for $\mathcal{O}(1)$ $flavour-independent$ CP phases. Although not particularly well motivated, this possibility is interesting since, when supplemented with a *real* non-trivial flavour structure, it allows for significant supersymmetric contributions to CP observables including those in the B system. In this case, the SM predictions can be significantly altered leading for instance to a nonclosure of the unitarity triangle (see M. Brhlik *et al.* in [23]). Given the appropriate A-terms' flavour structures, the parameters ε and ε' can be of completely supersymmetric nature [23]. Large flavour-independent SUSY phases may also be responsible for electroweak baryogenesis [35]. Thus the cancellation scenario presents a interesting alternative to the decoupling and approximate CP solutions.

For the case of the electron, the EDM cancellations occur between the chargino and the neutralino contributions. For the case of the neutron and mercury, there are cancellations between the gluino and the chargino contributions as well as cancellations among contributions of different quarks to the total EDM. A number of approximate formulae quantifying the cancellations are presented in Refs.[7],[36].

In what follows we examine the cancellation scenario in the universal and nonuniversal cases, with the latter being motivated by Type I string models. We note that the CP phases are to be understood modulo π.

4.3.1 EDM cancellations in mSUGRA-type models.

These are mSUGRA-type models allowing different phases for different gaugino masses while keeping their magnitudes the same. As we will see, mSUGRA models with zero gaugino phases can realize the cancellation scenario. An introduction of the gaugino phases makes the cancellations much harder to achieve (if possible at all) and leads to a much higher degree of fine-tuning. The parameters allowing the EDM cancellations strongly depend on the neutron model. For example, in the parton model, it is more difficult to achieve these cancellations due to the large strange quark contribution. Therefore, one cannot restrict the parameter space in a model-independent way and caution is needed when dealing with the parameters allowed by the cancellations.

In mSUGRA, the EDM cancellations can occur simultaneously for the electron,

neutron, and mercury along a band in the (ϕ_A, ϕ_μ) plane (Figs.10 and 11). However, in this case the mercury constraint requires the μ phase to be $\mathcal{O}(10^{-2})$ and the magnitude of the A-terms to be suppressed ($\sim 0.1 m_0$) which results in only a small effect of the A-terms on the phase of the corresponding mass insertion. This is to be contrasted with simultaneous EEDM/NEDM cancellations which allow for $\phi_\mu \sim \mathcal{O}(10^{-1})$ and $A \sim m_0$ [11],[36]. In that case the individual contributions to the EDMs exceeded the experimental limit by an order of magnitude (or more). Owing to the addition of the mercury constraint, the EDM cancellations become much milder as illustrated in Fig.12. For example, without these cancellations the EDMs would exceed the experimental limit only by a factor of a few. Obviously, the border between the cancellation and the small phases scenarios becomes blurred. This is even more so at larger $\tan\beta$ (Fig.13), in which case the cancellation band becomes narrower and the limits on ϕ_μ become tighter. We note that there could exist some points which allow for $\phi_\mu \sim \mathcal{O}(10^{-1})$ [38], however these are rare exceptions and such points do not form a band.

As noted in Ref.[11], in the case of zero gaugino phases, the band in the (ϕ_A, ϕ_μ) plane where the cancellations occur can approximately be described by a relation

$$\phi_\mu \simeq -a \sin\phi_A \ , \tag{36}$$

where a is a constant depending on the parameters of the model which represents the maximal allowed phase ϕ_μ. For example, for the chiral quark neutron model and $\tan\beta = 3$, $m_0 = m_{1/2} = 200$ GeV, and $|A| = 40$ GeV (parameters of Fig.10), $a = 0.017$. Of course, the value of a depends on the input parameters such as the quark masses, the GUT scale, the SUSY scale, etc. and also involves numerical uncertainties, so caution is needed when treating this number. The maximal allowed ϕ_μ is roughly inversely proportional to $\tan\beta$, e.g. for $\tan\beta = 10$ we have $a = 0.005$ (Fig.13). In the case of the parton model, the cancellations occur, for example, with $a = 0.006$ and $\tan\beta = 3$, $m_0 = m_{1/2} = 200$ GeV, and $|A| = 20$ GeV (Fig.11). As mentioned earlier, the cancellations are harder to achieve in the parton model, which results in tighter limits on ϕ_μ ($\sim \mathcal{O}(10^{-3})$). In both cases ϕ_μ is restricted to be of order $10^{-3} - 10^{-2}$, whereas ϕ_A can be arbitrary (however physical effects due to ϕ_A will be suppressed because of the small magnitude of A). The GUT parameters given above imply that the squark masses at low energies are about 500 GeV, so these bounds can be relaxed only if the squark masses are over 1 TeV.

If the gluino phase is turned on, simultaneous EEDM, NEDM, and mercury EDM cancellations are not possible. The gluino phase affects the NEDM cancellation band by altering the relation (36):

$$\phi_\mu \simeq -a \sin(\phi_A + \alpha) - c \ , \tag{37}$$

while leaving the EEDM cancellation band almost intact (Fig.14). An introduction of the bino phase ϕ_1 qualitatively has the same "off-setting" effect on the EEDM cancellation band as the gluino phase does on that of the NEDM (Fig.15). Note that the bino phase has no significant effect on the neutron and mercury cancellation bands since the neutralino contribution in both cases is small. When both the gluino and

bino phases are present (and fixed), simultaneous electron, neutron, and mercury EDMs cancellations do not appear to be possible along a band. The reason is that the mercury EDM depends on ϕ_3 more strongly than the NEDM does, so that an introduction of the gluino phase splits the bands where the mercury and neutron EDM cancellations occur as illustrated in Figs.14 and 15. Thus we see that zero gaugino phases are much more preferred by the cancellation scenario.

The cancellation scenario involves a significant fine-tuning. Indeed, restricting the phases to the band where the cancellations occur does not increase the symmetry of the model and thus is unnatural according to the t'Hooft's criterion [25]. It is a non-trivial task to quantify the degree of fine-tuning in this case. One possibility is to define an EDM sensitivity coefficient with respect to the CP-phases, in analogy with Eq.34. We typically find it to be between 30 and 100 on the cancellation band. This however represents only a local behaviour of the EDMs. In other words it shows how easy it is to spoil the cancellations without a reference to how improbable it is to achieve such cancellations in the first place. An alternative way to quantify the degree of fine-tuning is simply to estimate the probability that a random small area in the (ϕ_μ, ϕ_A) plane will safisfy the cancellation condition. Since any point is not prefered over any other point by the underlying theory, this should give a fairly good idea of the *minimal* degree of fine-tuning needed. From Fig.10 we obtain

$$\text{fine} - \text{tuning} \ \sim \ (\text{probability})^{-1} \ \gtrsim \ 10^2 \ . \tag{38}$$

Note that this estimate does not take into account the fine-tuning of the other soft breaking parameters which is necessary to allow for simultaneous EEDM, NEDM, and mercury EDM cancellations. Other estimates give a similar number for the universal case, whereas for the nonuniversal case the degree of fine-tuning drastically *increases*: only one out of 10^5 random points in the parameter space satisfies the cancellation condition [38].

4.3.2 EDM cancellations in D-brane models.

Let us first briefly review basic ideas of D-brane models (see also Refs.[39] and [40]). Recent studies of type I strings have shown that it is possible to construct a number of models with non–universal soft SUSY breaking terms which are phenomenologically interesting. Type I models can contain 9-branes, 5_i-branes, 7_i-branes, and 3-branes where the index $i = 1, 2, 3$ denotes the complex compact coordinate which is included in the 5-brane world volume or which is orthogonal to the 7-brane world volume. However, to preserve $N = 1$ supersymmetry in $D = 4$ not all of these branes can be present simultaneously and we can have (at most) either D9-branes with $D5_i$-branes or D3-branes with $D7_i$-branes.

Gauge symmetry groups are associated with stacks of branes located "on top of each other". A stack of N branes corresponds to the group $U(N)$. The matter fields are associated with open strings which start and end on the branes. These strings may be attached to either the same stack of branes or two different sets of branes which have overlapping world volumes. The ends of the string carry quantum numbers

associated with the symmetry groups of the branes. For example, the quark fields have to be attached to the $U(3)$ set of branes, while the quark doublet fields also have to be attached to the $U(2)$ set of branes. Given a brane configuration, the Standard Model fields are constructed according to their quantum numbers.

The SM gauge group can be obtained in the context of D-brane scenarios from $U(3) \times U(2) \times U(1)$, where the $U(3)$ arises from three coincident branes, $U(2)$ arises from two coincident D-branes and $U(1)$ from one D-brane. As explained in detail in Ref.[40], there are different possibilities for embedding the SM gauge groups within these D-branes. It was shown that if the SM gauge groups come from the same set of D-branes, one cannot produce the correct values for the gauge couplings $\alpha_j(M_Z)$ and the presence of additional matter (doublets and triplets) is necessary to obtain the experimental values of the couplings [41]. On the other hand, the assumption that the SM gauge groups originate from different sets of D-branes leads in a natural way to intermediate values for the string scale $M_S \simeq 10^{10-12}$ GeV [40]. In this case, the analysis of the soft terms has been done under the assumption that only the dilaton and moduli fields contribute to supersymmetry breaking and it has been found that these soft terms are generically non–universal. The MSSM fields arising from open strings are shown in Fig.3. For example, the up quark singlets u^c are states of the type C^{95_3}, the quark doublets are C^{95_1}, etc. The presence of extra (D_q) branes which are not associated with the SM gauge groups is often necessary to reproduce the correct hypercharge and to cancel non-vanishing tadpoles.

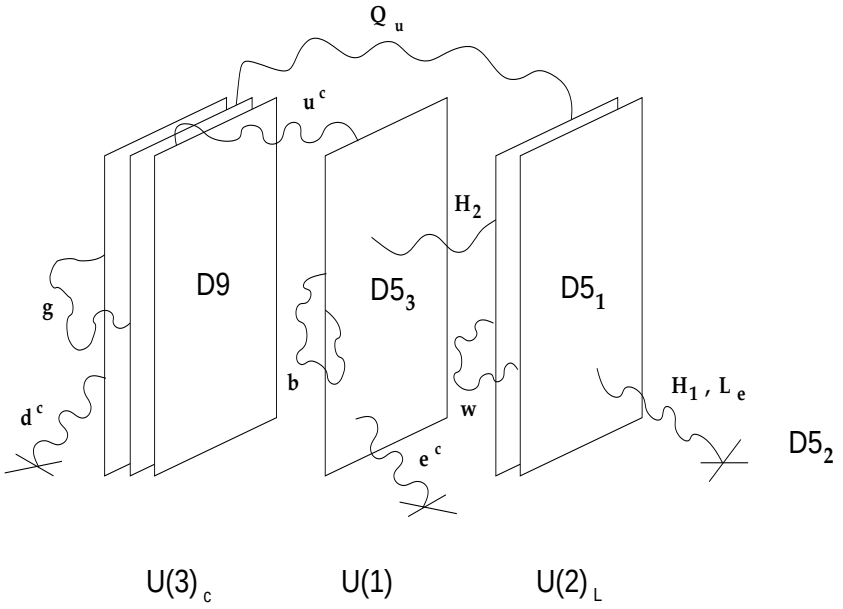


Figure 3: Embedding the SM gauge group within different sets of D-branes. The extra D_q brane (5_2) is marked by a cross.

Recently there has been a considerable interest in supersymmetric models derived from D-branes [42],[43]. In a toy model of Ref.[42], the gauge group $SU(3)_c \times U(1)_Y$

was associated with 5_1 branes and $SU(2)_L$ was associated with 5_2 branes. It was shown that in this model the gaugino masses are non–universal ($M_1 = M_3 \neq M_2$) so that the physical CP phases are $\phi_1 = \phi_3$, ϕ_A and ϕ_μ. Non-universality of the gaugino masses allowed to enlarge the regions of the parameter space where the NEDM/EEDM cancellations occured. However, such a model is oversimplified and the relation $\phi_1 = \phi_3 \neq \phi_2$ does not appear to hold in more realistic models [44]. In what follows we will consider the EDM cancellations in this and a more realistic D-brane models.

The model in which $U(3)$, $U(2)$, and $U(1)$ originate from different sets of branes is phenomenologically interesting. In this case one naturally obtains an intermediate string scale ($10^{10} - 10^{12}$ GeV), although higher values up to 10^{16} GeV are still allowed. Both the up and the down type Yukawa interactions are allowed, while that for the leptons typically vanishes (depending on further details of the model) [40]. The (anomaly-free) hypercharge is expressed in terms of the $U(1)$ charges $Q_{1,2,3}$ of the $U(1)_{1,2,3}$ groups:

$$Y = -\frac{1}{3}Q_3 - \frac{1}{2}Q_2 + Q_1 \ , \tag{39}$$

with the following (Q_3, Q_2, Q_1) charge assignment:

$$\begin{aligned} &q = (1,-1,0) \ , \ u^c = (-1,0,-1) \ , \ d^c = (-1,0,0) \ , \\ &l = (0,1,0) \ , \ e^c = (0,0,1) \ , \\ &H_2 = (0,1,1) \ , \ H_1 = (0,1,0) \ . \end{aligned} \tag{40}$$

The gaugino masses in this model are given by

$$\begin{aligned} M_3 &= \sqrt{3} m_{3/2} \sin\theta \ e^{-i\alpha_s} \ , \\ M_2 &= \sqrt{3} m_{3/2} \ \Theta_1 \cos\theta \ e^{-i\alpha_1} \ , \\ M_Y &= \sqrt{3} m_{3/2} \ \alpha_Y(M_S) \\ &\times \ \left(\frac{2}{\alpha_1(M_S)} \Theta_3 \cos\theta e^{-i\alpha_3} + \frac{1}{\alpha_2(M_S)} \Theta_1 \cos\theta e^{-i\alpha_1} + \frac{2}{3\alpha_3(M_S)} \sin\theta e^{-i\alpha_s} \right) \ , \end{aligned} \tag{41}$$

where

$$\frac{1}{\alpha_Y(M_S)} = \frac{2}{\alpha_1(M_S)} + \frac{1}{\alpha_2(M_S)} + \frac{2}{3\alpha_3(M_S)} \ . \tag{42}$$

Here α_k correspond to the gauge couplings of the $U(k)$ branes. As shown in Ref.[40], $\alpha_1(M_S) \simeq 0.1$ leads to the string scale $M_S \approx 10^{12}$ GeV. The parameters θ and Θ_i parameterize supersymmetry breaking in the usual way [39]:

$$\begin{aligned} F^S &= \sqrt{3}(S + S^*) m_{3/2} \sin\theta \ e^{-i\alpha_s} \ , \\ F^i &= \sqrt{3}(T_i + T_i^*) m_{3/2} \cos\theta \ \Theta_i e^{-i\alpha_i} \ , \end{aligned} \tag{43}$$

and $i = 1, 2, 3$ labels the three complex compact dimensions.

The soft scalar masses are given by

$$m_q^2 \ = \ m_{3/2}^2 \left[1 - \frac{3}{2} \left(1 - \Theta_1^2 \right) \cos^2\theta \right] \ ,$$

$$
\begin{aligned}
m^2_{d^c} &= m^2_{3/2}\left[1-\frac{3}{2}\left(1-\Theta_2^2\right)\cos^2\theta\right] \ , \\
m^2_{u^c} &= m^2_{3/2}\left[1-\frac{3}{2}\left(1-\Theta_3^2\right)\cos^2\theta\right] \ , \\
m^2_{e^c} &= m^2_{3/2}\left[1-\frac{3}{2}\left(\sin^2\theta+\Theta_1^2\cos^2\theta\right)\right] \ , \\
m^2_{l} &= m^2_{3/2}\left[1-\frac{3}{2}\left(\sin^2\theta+\Theta_3^2\cos^2\theta\right)\right] \ , \\
m^2_{H_2} &= m^2_{3/2}\left[1-\frac{3}{2}\left(\sin^2\theta+\Theta_2^2\cos^2\theta\right)\right] \ , \\
m^2_{H_1} &= m^2_{l} \ , \qquad (44)
\end{aligned}
$$

and the trilinear parameters are

$$
\begin{aligned}
A_u &= \frac{\sqrt{3}}{2}m_{3/2}\left[\left(\Theta_2 e^{-i\alpha_2}-\Theta_1 e^{-i\alpha_1}-\Theta_3 e^{-i\alpha_3}\right)\cos\theta-\sin\theta\ e^{-i\alpha_s}\right] \ , \qquad (45) \\
A_d &= \frac{\sqrt{3}}{2}m_{3/2}\left[\left(\Theta_3 e^{-i\alpha_3}-\Theta_1 e^{-i\alpha_1}-\Theta_2 e^{-i\alpha_2}\right)\cos\theta-\sin\theta\ e^{-i\alpha_s}\right] \ , \qquad (46) \\
A_e &= 0 \ . \qquad (47)
\end{aligned}
$$

We observe that the angles Θ_i and θ are quite constrained if we are to avoid negative mass-squared's for squarks and sleptons. In what follows we set $\Theta_3 = 0$ and $\alpha_1 = \alpha_2$; then the soft terms are parameterized in terms of the phase $\phi \equiv \alpha_1 - \alpha_s$.

In Fig.16 we display the bands allowed by the electron (red), neutron (green), and mercury (blue) EDMs. In this figure, we set $m_{3/2} = 150$ GeV, $\tan\beta = 3$, $\Theta_1^2 = \Theta_2^2 = 1/2$, $\cos^2\theta = 2\sin^2\theta = 2/3$, and $\alpha_1(M_S) \sim 1$ with M_S being the GUT scale. For the plot to be more illustrative, we do not impose any additional constraints besides the EDM ones (i.e. bounds on the chargino and slepton masses, etc.). It is clear that even though simultaneous EEDM/NEDM cancellations allow the phase ϕ to be $\mathcal{O}(1)$, an addition of the mercury constraint requires all phases to be very small (modulo π) and thus practically rules out the cancellation scenario in this context. The situation becomes even worse in the case of an intermediate string scale $\sim 10^{12}$ GeV (i.e. $\alpha_1(M_S) \sim 0.1$), see Fig.17. We find it quite generic that the mercury EDM behaviour in D-brane models is very different from that of the electron and neutron and thus is crucial in constraining the parameter space. The major difference from the mSUGRA-type models with fixed ϕ_Y and ϕ_3 is that the phase of the A-terms is correlated with the gaugino phases resulting in the cancellation bands which are not described by a simple relation $\phi_\mu \simeq -a\sin(\phi_A+\alpha)-c$.

Next we consider the model of Ref.[42]. The (corrected) soft terms for this model read (for $\Theta_3 = 0$)

$$
\begin{aligned}
& M_Y = M_3 = -A = \sqrt{3}m_{3/2}\cos\theta\ \Theta_1 e^{-i\alpha_1} \ , \\
& M_2 = \sqrt{3}m_{3/2}\cos\theta\ \Theta_2 e^{-i\alpha_2} \ , \\
& m_L^2 = m_{3/2}^2(1-\frac{3}{2}\sin^2\theta); \\
& m_R^2 = m_{3/2}^2(1-3\cos^2\theta\ \Theta_2^2) \ . \qquad (48)
\end{aligned}
$$

To illustrate the EDM constraints, we choose the parameters which allow for simultaneous EEDM/NEDM cancellations, namely $m_{3/2} = 150$ GeV, $\tan\beta = 2$, $\Theta_1 = 0.9$, and $\theta = 0.4$ as given in Ref.[42]. Fig.18 shows that the mercury constraint has the same behaviour as in the model considered above and rules out large CP-phases.

We see that the cancellation scenario in simple models faces a number of difficulties. Presently available string-motivated models with non-universal gaugino masses cannot accommodate simultaneous electron, neutron, and mercury EDM cancellations. In the mSUGRA, such cancellations are possible but require a significant fine-tuning. The addition of the mercury EDM bound restricts the phase of the μ term to be $\mathcal{O}(10^{-2})$ if we are to achieve the EDM cancellations along a band in the (ϕ_A, ϕ_μ) plane. Without an additional SUSY flavour structure, the CP-phases allowed by the cancellations will have very small observable effects. Even in a more general situation (unconstrained MSSM), the phases allowed by the EDM cancellations typically lead to small CP-asymmetries ($\lesssim 1\%$) in collider experiments [38]. Testing the cancellation scenario experimentally may prove to be a challenge.

4.4 Flavour-off-diagonal CP violation

This is one of the more attractive possibilities to avoid overproduction of EDMs in SUSY models. Nonobservation of EDMs may imply that CP-violation has a flavour-off-diagonal character just like in the Standard Model. The origin of CP-violation in this case is closely related to the origin of the flavour structures rather than the origin of supersymmetry breaking. While models with flavour-off-diagonal CP violation naturally avoid the EDM problem, they have testable effects in K and B physics.

This class of models requires hermitian Yukawa matrices and A-terms, which forces the flavour-diagonal phases to vanish (up to small RG corrections) in any basis. The flavour-independent quantities such as the μ-term, gaugino masses, etc. are real. This is naturally implemented in left-right symmetric models [45] and models with a horizontal flavour symmetry [47].

In the left-right models, the hermiticity of the Yukawas and A-terms as well as the reality of the μ-term is forced by the left-right symmetry. The $SU(2)_L$ gaugino mass is in general complex, so in order to suppress the EDMs the additional assumption of its reality is needed. The phenomenology of such models in the context of up-down unification has been studied in [46]. The left-right symmetry appears to be too restrictive in this case to satisfy all of the phenomenological constraints; however the decisive test will be undertaken at the B factories.

Another possibility is based on a horizontal $U(3)_H$ symmetry [47]. Hermitian Yukawa matrices may appear due to a (gauged) horizontal symmetry $U(3)_H$ which gets broken spontaneously by the VEVs of the real adjoint fields T^a_α ($a = 1..9$; $\alpha = u, d, l, ..$) [48]. Some of these *real* VEV's also break CP since some of the components of T^a_α are CP-odd. As a result, CP violation appears in the superpotential through complex Yukawa couplings, whereas the μ-term is real since it arises from a $U(3)_H$ invariant combination of the type $T^a_\alpha T^a_\beta$. An effective $U(3)_H$-invariant superpotential of the type $\hat{W} = \frac{g_H}{M}\hat{H}_1\hat{Q}_i(T^a_d\lambda^a)_{ij}\hat{D}_j$ produces the Yukawa matrix $(Y^d)_{ij} = \frac{g_H}{M}\langle T^a_d\rangle(\lambda^a)_{ij}$, where

λ^0 is proportional to the unit matrix and λ^{1-8} are the Gell-Mann matrices. Note that the *real* fields T^a_α may only come from a non-supersymmetric (anti-brane) sector. If T^a_α are the scalar components of chiral multiplets, they are intrinsically complex and hermitian Yukawas in this case arise only if the VEVs of T^a_α are real.

The gaugino masses in this model are not forced to be real by symmetry. One has to make an additional assumption that either the gaugino masses are universal and the corresponding phase can be rotated away or that the SUSY breaking dynamics conserve CP which seems natural if CP breaking is associated with the origin of flavour structures. In other words, the SUSY breaking auxiliary fields get real VEVs as a result of the underlying dynamics such as the dilaton stabilization in Type I string models [49] or the effective potential minimization in heterotic string models [50]. Further, if the Kähler potential is either generation independent or left-right symmetric, the A-terms are hermitian [47]. This leads to very small phases in the flavour-diagonal mass insertions which are responsible for generating EDMs and the EDM bounds are easily satisfied.

Both the left-right model and the model with a horizontal symmetry mitigate the strong CP-problem (under the additional assumptions given above). The $\bar{\theta}$ parameter vanishes at both the tree and the leading log one-loop levels. However neither of these models solves the problem completely due to the significant one loop finite corrections which appear mostly due to a non-degeneracy of the squark masses and a misalignment between the Yukawas and the A-terms [51].

In this class of models we have the following setting at the high energy scale:

$$\begin{aligned} &Y_\alpha = Y_\alpha^\dagger \, , A_\alpha = A_\alpha^\dagger \, , \\ &\mathrm{Arg}(M_k) = \mathrm{Arg}(\mu) = 0 \, . \end{aligned} \tag{49}$$

Generally, the off-diagonal elements of the A-terms can have $\mathcal{O}(1)$ phases without violating the EDM constraints. Due to the RG effects, large phases in the soft trilinear couplings involving the third generation generate small phases in the flavour-diagonal mass insertions for the light generations, and thus induce the EDMs. For example, the A-terms of the form[3]

$$A_d = A_u = m_0 \begin{pmatrix} 1 & a_{12} & a_{13} \\ a_{12}^* & 1 & a_{23} \\ a_{13}^* & a_{23}^* & a_{33} \end{pmatrix} \tag{50}$$

and the following GUT-scale hermitian Yukawa matrices

$$Y^u = \begin{pmatrix} 4.1 \times 10^{-4} & 6.9 \times 10^{-4}\,\mathrm{i} & -1.4 \times 10^{-2} \\ -6.9 \times 10^{-4}\,\mathrm{i} & 3.5 \times 10^{-3} & -1.4 \times 10^{-5}\,\mathrm{i} \\ -1.4 \times 10^{-2} & 1.4 \times 10^{-5}\,\mathrm{i} & 6.9 \times 10^{-1} \end{pmatrix} \, ,$$

$$Y^d = \begin{pmatrix} 1.3 \times 10^{-4} & 2.0 \times 10^{-4} + 1.8 \times 10^{-4}\,\mathrm{i} & -4.4 \times 10^{-4} \\ 2.0 \times 10^{-4} - 1.8 \times 10^{-4}\,\mathrm{i} & 9.3 \times 10^{-4} & 7.0 \times 10^{-4}\,\mathrm{i} \\ -4.4 \times 10^{-4} & -7.0 \times 10^{-4}\,\mathrm{i} & 1.9 \times 10^{-2} \end{pmatrix} \, .$$

[3]The standard supergravity relation $(\hat{A}_\alpha)_{ij} = (A_\alpha)_{ij}(Y_\alpha)_{ij}$ for the trilinear soft couplings is assumed.

typically induce the mercury EDM of the order of the experimental limit if a_{33} is of order 1, whereas the induced NEDM is 1-2 orders of magnitude below the experimental limit. If one uses Yukawa textures with smaller Y^{α}_{13}, this RG effect will be suppressed rendering the induced mercury EDM far below the experimental limit.

The supersymmetric contribution to the ε' parameter is suppressed in models with hermitian flavour structures[4] [47]. This occurs due to severe cancellations between the contributions involving $(\delta^d_{12})_{LR}$ and $(\delta^d_{12})_{RL}$ mass insertions (we use the standard definitions of [53]). Due to the hermiticity $(\delta^d_{12})_{LR} \simeq (\delta^d_{12})_{RL}$, whereas they contribute to ε' with opposite signs. Typically we find $\left|\mathrm{Im}\left[(\delta^d_{12})_{LR} - (\delta^d_{12})_{RL}\right]\right| < 10^{-6}$ which produces ε' an order of magnitude below the experimental limit [53]. On the other hand, similar cancellations do not occur for the ε parameter and the SUSY contribution to ε can be even dominant. The value of $(\delta^d_{12})_{LR}$ which saturates the observed $|\varepsilon| \simeq 2.26 \times 10^{-3}$ is given by $\sqrt{|\mathrm{Im}(\delta^d_{12})^2_{LR}|} \simeq 3.5 \times 10^{-4}$ for the gluino and squark masses of 500 GeV [53].

For completeness, we provide the bounds on the imaginary parts of the mass insertions

$$(\delta^{d(u)}_{ii})_{LR} = \frac{1}{\tilde{m}^2}((\hat{A}^{d(u)\dagger}_{SCKM})_{ii} v_{1(2)} - Y^{d(u)}_i \mu v_{2(1)}) \tag{51}$$

derived from the leading gluino contributions to the electromagnetic (NEDM) operator and the bino contribution to the electron EDM. We update the bounds of Ref.[53] and also include the QCD correction factor. The advantage of the mass insertion approach is that it allows to obtain model independent bounds and thus is quite useful when dealing with complicated flavour structures. For comparison we present the bounds for the chiral (Table 1) and the parton (Table 2) neutron models.

A drastic improvement of the bounds comes from the addition of the mercury EDM constraint. Using the expressions for the chromomagnetic moments of Ref.[37], in Table 3 we present the bounds on the mass insertions from the gluino contributions to the mercury EDM. For $|\mathrm{Im}(\delta^d_{11})_{LR})|$ and $|\mathrm{Im}(\delta^u_{11})_{LR})|$ these bounds turn out to be very strict, more than an order of magnitude stricter than those imposed by the NEDM. This severely restricts the CP-asymmetry $A_{CP}(b \to s\gamma)$ in models with hermitian flavour structures. The reason is that in order to obtain a large ($\sim 10\%$) SUSY contribution to this observable, the elements of the A-terms involving the third generation have to be larger than 1. This induces via the RG running a considerable $|\mathrm{Im}(\delta^{d,u}_{11})_{LR})|$, often in conflict with the bounds of Table 3. We find that with the above Yukawa textures $A_{CP}(b \to s\gamma)$ is allowed to be no more than 2-3%. One can relax this constraint by using different hermitian textures, especially with suppressed Y^{α}_{13}. In this case the CP-asymmetry can be as large as 6-7%.

To conclude this section, we remark that the problem of baryogenesis in this class of models requires careful investigation and at the moment it is unclear whether or not large flavour off-diagonal SUSY phases can produce sufficient baryon asymmetry of the universe.

[4]For phenomenology of models with non-universal (but non-hermitian) A-terms see also [52].

5 Discussion and conclusions

We have systematically analyzed constraints on supersymmetric models imposed by the experimental bounds on the electron, neutron, and mercury electric dipole moments. We find that the EDMs can be suppressed in SUSY models with

1) small SUSY CP-phases ($\lesssim 10^{-2}$). This possibility can be motivated by the approximate CP-symmetry which also implies that the CKM phase is small. This provides testable signatures for B-factories' experiments.

2) heavy SUSY scalars, $m_{sfermion} \sim 10$ TeV. In this class of models there is a large hierarchy between the SUSY and electroweak scales, which is hard to realize without an extreme fine-tuning.

3) EDM cancellations. We have analyzed the possibility of such cancellations in D-brane and mSUGRA-like models with nontrivial gaugino phases. We find that, with the addition of the mercury EDM constraint, only the EDM cancellations in mSUGRA ($\phi_1 \simeq \phi_3 \simeq 0$) survive in any considerable part of the parameter space. Even in this case the cancellations require small $\phi_\mu \sim 10^{-2}$ and suppressed $|A|$ ($\sim 0.1 m_0$). As a result, the border between the small phases and the cancellation scenarios fades away. In addition to the finetuning problem, models with the EDM cancellations lack predictive power as it is unclear whether the allowed CP-phases can have observable effects.

4) flavour-off-diagonal CP violation. This can occur in models with CP-conserving SUSY breaking dynamics and hermitian flavour structures. Such models allow for $\mathcal{O}(1)$ flavour off-diagonal phases which can have significant effects in K and B physics.

It is also possible to combine different mechanisms to suppress the EDMs. For example, a "hybrid" of the decoupling and the cancellation scenarios was considered in Ref.[54]. Such models seem to share shortcomings of both "parents" without an apparent advantage over either of them.

There is also a rather radical proposal that all gaugino masses and the A-terms are vanishingly small [55]. Clearly this eliminates all of the physical phases in Eq.(15) and thus produces no CP violation. Such a strong assumption requires a firm motivation such as the continuous R-symmetry. However, by the same token, the R-symmetry eliminates the $B\mu$ term thereby leading to a very light CP-odd Higgs boson. Such a scenario faces a number of difficulties with experimental results.

To summarize, we have studied the supersymmetric CP problem taking into account all of the current EDM constraints. Our conclusion is that there remain two attractive ways to avoid overproduction of the EDMs in SUSY models. The first possibility is that CP is an approximate symmetry of nature and the second one is that CP violation has a flavour off-diagonal character just as in the Standard Model.

Acknowledgements. S.A. and O.L. were supported by the PPARC Opportunity grant, S.K. was supported by the PPARC SPG. The authors are grateful to D. Bailin, M. Brhlik, T. Ibrahim, C. Muñoz, and M. Pospelov for useful discussions, and to M. Gomez and D. Cerdeño for their help in the computing aspects of this work.

References

[1] T. Affolder *et al.*, CDF collaboration, Phys. Rev. **D61** (2000), 072005; B. Aubert *et al.*, BaBar collaboration, hep-ex/0102030 ; A. Abashian *et al.*, Belle collaboration, hep-ex/0102018.

[2] P.G. Harris *et al.*, Phys. Rev. Lett. **82** (1999), 904; see also the discussion in S.K. Lamoreaux and R. Golub, Phys. Rev. **D61** (2000), 051301.

[3] E.D. Commins *et al.*, Phys. Rev. **A50** (1994), 2960.

[4] M.V. Romalis, W.C. Griffith, and E.N. Fortson, Phys. Rev. Lett. **86**, 2505 (2001); J.P. Jacobs *et al.*, Phys. Rev. Lett. **71** (1993), 3782.

[5] T. Falk, K.A. Olive, M. Pospelov, R. Roiban, Nucl. Phys. **B560** (1999), 3.

[6] H. Georgi and A. Manohar, Nucl. Phys. **B234**, 189 (1984); R. Arnowitt, J.L. Lopez and D.V. Nanopoulos, Phys. Rev. **D42** (1990), 2423; R. Arnowitt, M.J. Duff and K.S. Stelle, Phys. Rev. **D43** (1991), 3085.

[7] T. Ibrahim and P. Nath, Phys. Rev. **D57** (1998), 478; Errata-*ibid.* **D58**, 019901 (1998); *ibid.* **D60**, 019901 (1999); Phys. Lett. **B418**, 98 (1998); Phys. Rev. **D58**, 111301 (1998); Erratum-*ibid.* **D60**, 099902 (1999).

[8] M. Pospelov and A. Ritz, Phys. Rev. D **63**, 073015 (2001).

[9] V.M. Khatsimovsky, I.B. Khriplovich and A.R. Zhitnitsky, Z. Phys. **C36** (1987), 455; V.M. Khatsimovsky, I.B. Khriplovich and A.S. Yelkhovsky, Annals Phys. **186** (1988), 1; V.M. Khatsimovsky and I.B. Khriplovich, Phys. Lett. **B296** (1992), 219.

[10] J. Ellis, R. Flores, Phys. Lett. **B377** (1996), 83.

[11] A. Bartl, T. Gajdosik, W. Porod, P. Stockinger, and H. Stremnitzer, Phys. Rev. **D60** (1999), 073003.

[12] W. Fischler, S. Paban and S. Thomas, Phys. Lett. B **289**, 373 (1992).

[13] I.B. Khriplovich and S.K. Lamoreaux, *"CP Violation Without Strangeness"*, Springer, 1997.

[14] S. Weinberg, Phys. Rev. Lett. **63**, 2333 (1989); E. Braaten, C. Li and T. Yuan, Phys. Rev. Lett. **64**, 1709 (1990).

[15] J. Dai, H. Dykstra, R. G. Leigh, S. Paban and D. Dicus, Phys. Lett. **B237**, 216 (1990).

[16] D. Chang, W. Keung and A. Pilaftsis, Phys. Rev. Lett. **82**, 900 (1999); Erratum-*ibid.* **83**, 3972 (1999).

[17] S. M. Barr and A. Zee, Phys. Rev. Lett. **65**, 21 (1990).

[18] J. F. Gunion and H. E. Haber, Nucl. Phys. **B272**, 1 (1986).

[19] S. Baek and P. Ko, Phys. Rev. Lett. **83**, 488 (1999).

[20] D. Chang, W. Chang and W. Keung, Phys. Lett. **B478**, 239 (2000); A. Pilaftsis, Phys. Lett. **B471**, 174 (1999).

[21] A. Pilaftsis, Phys. Rev. D **62**, 016007 (2000).

[22] M. Dine, E. Kramer, Y. Nir, Y. Shadmi, hep-ph/0101092; G. Eyal and Y. Nir, Nucl. Phys. **B528** (1998), 21; and references therein.

[23] A. Masiero and H. Murayama, Phys. Rev. Lett. **83** (1999), 907; S. Khalil and T. Kobayashi, Phys. Lett. B **460**, 341 (1999); M. Brhlik, L. Everett, G. L. Kane, S. F. King and O. Lebedev, Phys. Rev. Lett. **84** (2000), 3041.

[24] M. Carena, M. Quiros, A. Riotto, I. Vilja and C. E. Wagner, Nucl. Phys. B **503**, 387 (1997).

[25] G. 't Hooft, in *Recent Advances in Gauge Theories*, Proceedings of the Cargese Summer Institute, Cargese, France, 1979, edited by G. t' Hooft *et al.*, NATO Advanced Study Institute Series B; Physics Vol.59 (Plenum, New York, 1980).

[26] D. Bailin, G. V. Kraniotis and A. Love, Nucl. Phys. B **518**, 92 (1998); J. Giedt, Nucl. Phys. B **595**, 3 (2001); T. Dent, hep-th/0011294.

[27] P. Nath, Phys. Rev. Lett. **66** (1991), 2565; Y. Kizukuri and N. Oshimo, Phys. Rev. **D46** (1992) 3025.

[28] R. Barbieri and G.F. Giudice, Nucl. Phys. **B306** (1988), 63; J. Ellis, K. Enqvist, D.V. Nanopoulos, F. Zwirner, Mod. Phys. Lett. **A1** (1986), 57; G.G. Ross and R.G. Roberts, Nucl. Phys. **B377** (1992), 571.

[29] J.L. Feng, K.T. Matchev, and T. Moroi, Phys. Rev. **D61** (2000), 075005; Phys. Rev. Lett. **84** (2000), 2322.

[30] J. L. Feng, C. Kolda and N. Polonsky, Nucl. Phys. B **546**, 3 (1999).

[31] H. Baer, C. Balazs, M. Brhlik, P. Mercadante, X. Tata, Y. Wang, hep-ph/0102156.

[32] S. Dimopoulos and G. F. Giudice, Phys. Lett. **B357** (1995), 573.

[33] H. Baer, M. A. Diaz, P. Quintana and X. Tata, JHEP**0004**, 016 (2000).

[34] L. Everett, G.L. Kane, S. Rigolin, L.-T. Wang, hep-ph/0102145; J.L. Feng and K.T. Matchev, hep-ph/0102146; E.A. Baltz and P. Gondolo, hep-ph/0102147; U. Chattopadhyay and P. Nath, hep-ph/0102157.

[35] M. Brhlik, G. J. Good and G. L. Kane, Phys. Rev. D **63**, 035002 (2001).

[36] T. Falk and K.A. Olive, Phys. Lett. B **375**, 196 (1996); Phys. Lett. B **439**, 71 (1998); M. Brhlik, G.J. Good and G.L. Kane, Phys. Rev. D **59**, 115004 (1999).

[37] S. Pokorski, J. Rosiek and C.A. Savoy, Nucl. Phys. B **570**, 81 (2000).

[38] V. Barger, T. Falk, T. Han, J. Jiang, T. Li, and T. Plehn, hep-ph/0101106.

[39] L. E. Ibàñez, C. Muñoz and S. Rigolin, Nucl. Phys. B **553**, 43 (1999); A. Brignole, L. E. Ibàñez, and C. Muñoz, Nucl. Phys. B **422**, 125 (1994).

[40] D.G. Cerdeño, E. Gabrielli, S. Khalil, C. Muñoz, E. Torrente-Lujan, hep-ph/0102270, to appear in Nucl. Phys. **B**.

[41] G. Aldazabal, L. E. Ibàñez, F. Quevedo and A. M. Uranga, JHEP**0008**, 002 (2000); D. Bailin, G. V. Kraniotis and A. Love, hep-th/0011289.

[42] M. Brhlik, L. Everett, G.L. Kane and J. Lykken, Phys. Rev. Lett. **83**, 2124 (1999); M. Brhlik, L. Everett, G. L. Kane and J. Lykken, Phys. Rev. D **62**, 035005 (2000).

[43] E. Accomando, R. Arnowitt and B. Dutta, Phys. Rev. D **61**, 075010 (2000); T. Ibrahim and P. Nath, Phys. Rev. D **61**, 093004 (2000).

[44] S. Abel, S. Khalil, and O. Lebedev, hep-ph/0103031.

[45] R. N. Mohapatra and G. Senjanovic, Phys. Lett. **B79**, 283 (1978); R. N. Mohapatra and A. Rasin, Phys. Rev. Lett. **76**, 3490 (1996); Phys. Rev. **D 54**, 5835 (1996).

[46] K. S. Babu, B. Dutta and R. N. Mohapatra, Phys. Rev. **D 61**, 091701 (2000).

[47] S. Abel, D. Bailin, S. Khalil and O. Lebedev, hep-ph/0012145, to appear in Phys. Lett. **B**.

[48] A. Masiero and T. Yanagida, hep-ph/9812225.

[49] S. A. Abel and G. Servant, Nucl. Phys. B **597**, 3 (2001); S. A. Abel and G. Servant, *in preparation.*

[50] D. Bailin, G. V. Kraniotis and A. Love, Phys. Lett. B **432**, 343 (1998).

[51] M. Dine, R. G. Leigh and A. Kagan, Phys. Rev. D **48**, 2214 (1993).

[52] S.A. Abel and J.-M. Frére, Phys. Rev. D **55**, 1623 (1997); S. Khalil, T. Kobayashi and A. Masiero, Phys. Rev. D **60**, 075003 (1999); S. Khalil, T. Kobayashi and O. Vives, Nucl. Phys. B **580**, 275 (2000).

[53] F. Gabbiani, E. Gabrielli, A. Masiero and L. Silvestrini, Nucl. Phys. B **477**, 321 (1996).

[54] U. Chattopadhyay, T. Ibrahim and D. P. Roy, hep-ph/0012337.

[55] L. Clavelli, T. Gajdosik and W. Majerotto, Phys. Lett. **B494**, 287 (2000).

x	$\lvert\mathrm{Im}(\delta^d_{11})_{LR}\rvert$	$\lvert\mathrm{Im}(\delta^u_{11})_{LR}\rvert$	$\lvert\mathrm{Im}(\delta^l_{11})_{LR}\rvert$
0.1	1.0×10^{-6}	2.0×10^{-6}	1.4×10^{-7}
0.3	9.2×10^{-7}	1.8×10^{-6}	1.3×10^{-7}
1	1.1×10^{-6}	2.2×10^{-6}	1.6×10^{-7}
3	1.8×10^{-6}	3.6×10^{-6}	2.6×10^{-7}
5	2.4×10^{-6}	4.9×10^{-6}	3.5×10^{-7}
10	4.1×10^{-6}	8.2×10^{-6}	5.9×10^{-7}

Table 1: Bounds on the imaginary parts of the mass insertions. The chiral quark model for the neutron is assumed. Here $x = m^2_{\tilde{g}}/m^2_{\tilde{q}} = m^2_{\tilde{B}}/m^2_{\tilde{l}}$, $m_{\tilde{q}} = 500\ GeV, m_{\tilde{l}} = 100\ GeV$. For different squark/slepton masses the bounds are to be multiplied by $m_{\tilde{q}}/500\ GeV$ or $m_{\tilde{l}}/100\ GeV$.

x	$\lvert\mathrm{Im}(\delta^d_{11})_{LR}\rvert$	$\lvert\mathrm{Im}(\delta^u_{11})_{LR}\rvert$	$\lvert\mathrm{Im}(\delta^d_{22})_{LR}\rvert$
0.1	1.8×10^{-6}	1.3×10^{-6}	5.9×10^{-6}
0.3	1.6×10^{-6}	1.2×10^{-6}	5.4×10^{-6}
1	1.9×10^{-6}	1.5×10^{-6}	6.6×10^{-6}
3	3.2×10^{-6}	2.3×10^{-6}	1.1×10^{-5}
5	4.4×10^{-6}	3.2×10^{-6}	1.4×10^{-5}
10	7.3×10^{-6}	5.4×10^{-6}	2.4×10^{-5}

Table 2: Bounds on the imaginary parts of the mass insertions for the parton neutron model. For the squark masses different from 500 GeV, the bounds are to be multiplied by $m_{\tilde{q}}/500\ GeV$.

x	$\lvert\mathrm{Im}(\delta^d_{11})_{LR}\rvert$	$\lvert\mathrm{Im}(\delta^u_{11})_{LR}\rvert$	$\lvert\mathrm{Im}(\delta^d_{22})_{LR}\rvert$
0.1	2.6×10^{-8}	2.6×10^{-8}	2.2×10^{-6}
0.3	3.6×10^{-8}	3.6×10^{-8}	3.0×10^{-6}
1	6.7×10^{-8}	6.7×10^{-8}	5.6×10^{-6}
3	1.5×10^{-7}	1.5×10^{-7}	1.3×10^{-5}
5	2.5×10^{-7}	2.5×10^{-7}	2.1×10^{-5}
10	5.3×10^{-7}	5.3×10^{-7}	4.4×10^{-5}

Table 3: Bounds on the imaginary parts of the mass insertions imposed by the mercury EDM. For the squark masses different from 500 GeV, the bounds are to be multiplied by $m_{\tilde{q}}/500\ GeV$.

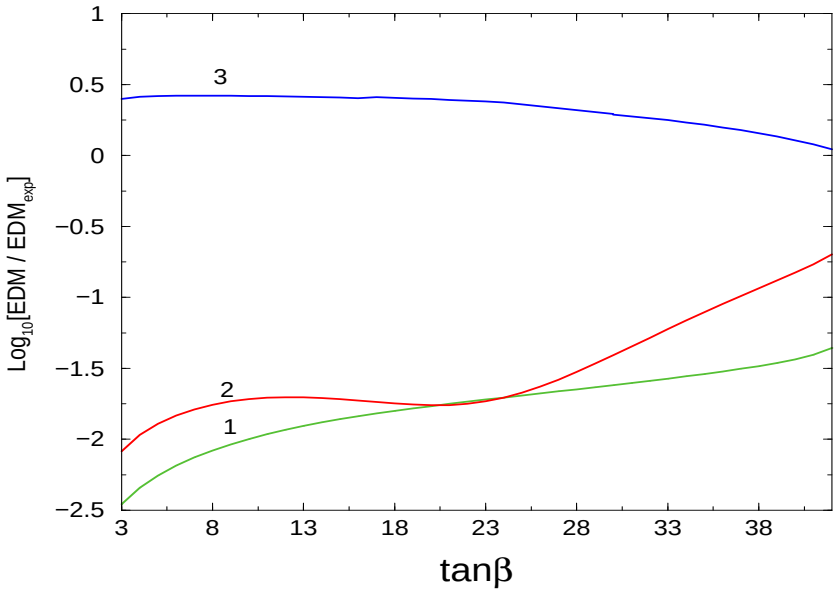


Figure 4: Barr-Zee and Weinberg operator induced EDMs as a function of $\tan\beta$. 1 – electron Barr-Zee EDM, 2 – neutron Barr-Zee EDM, 3 – neutron EDM due to the Weinberg operator. Here $m_0 = m_{1/2} = A = 200$ GeV, $\phi_\mu = 0$, $\phi_A = \pi/2$.

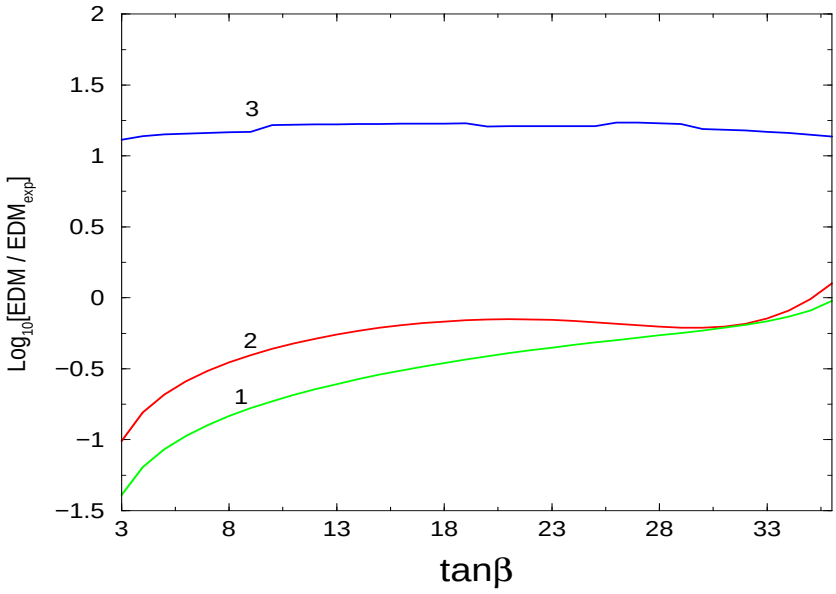


Figure 5: Barr-Zee and Weinberg operator induced EDMs as a function of $\tan\beta$. 1 – electron Barr-Zee EDM, 2 – neutron Barr-Zee EDM, 3 – neutron EDM due to the Weinberg operator. Here $m_0 = 500$ GeV, $m_{1/2} = 200$ GeV, $A = 600$ GeV, $\phi_\mu = 0$, $\phi_A = \pi/2$.

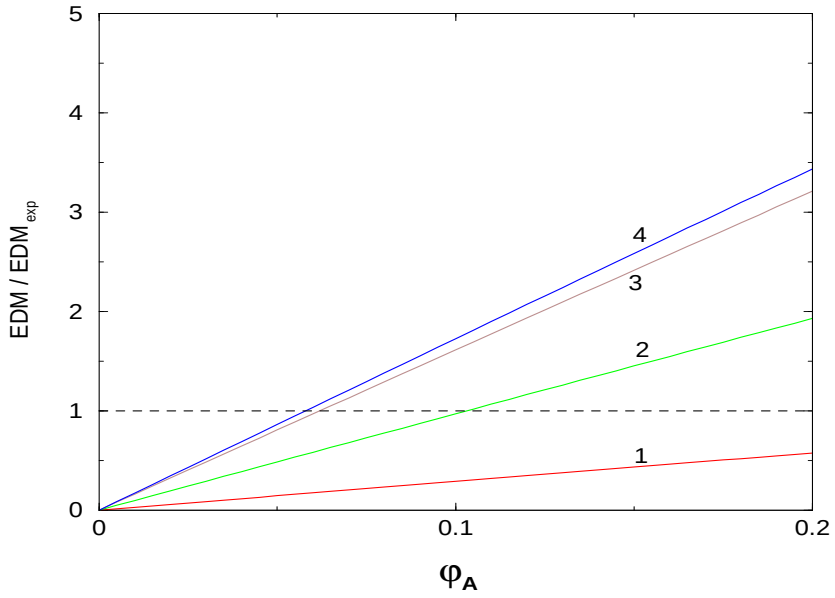


Figure 6: EDMs as a function of ϕ_A. 1 – electron, 2 – neutron (chiral model), 3 – neutron (parton model), 4 – mercury. The experimental limit is given by the horizontal line. Here $\tan\beta = 3$, $m_0 = m_{1/2} = A = 200$ GeV.

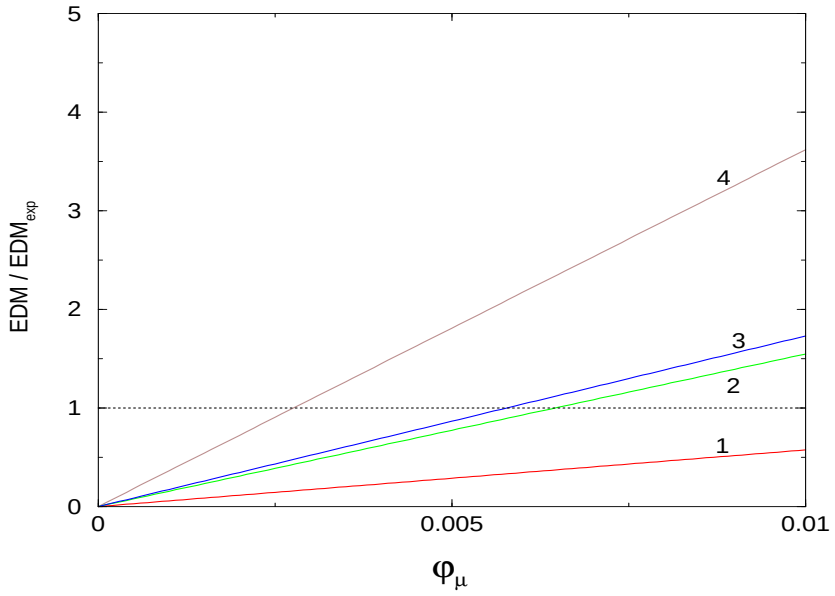


Figure 7: EDMs as a function of ϕ_μ. 1 – electron, 2 – neutron (chiral model), 3 – mercury, 4 – neutron (parton model). The experimental limit is given by the horizontal line. Here $\tan\beta = 3$, $m_0 = m_{1/2} = A = 200$ GeV.

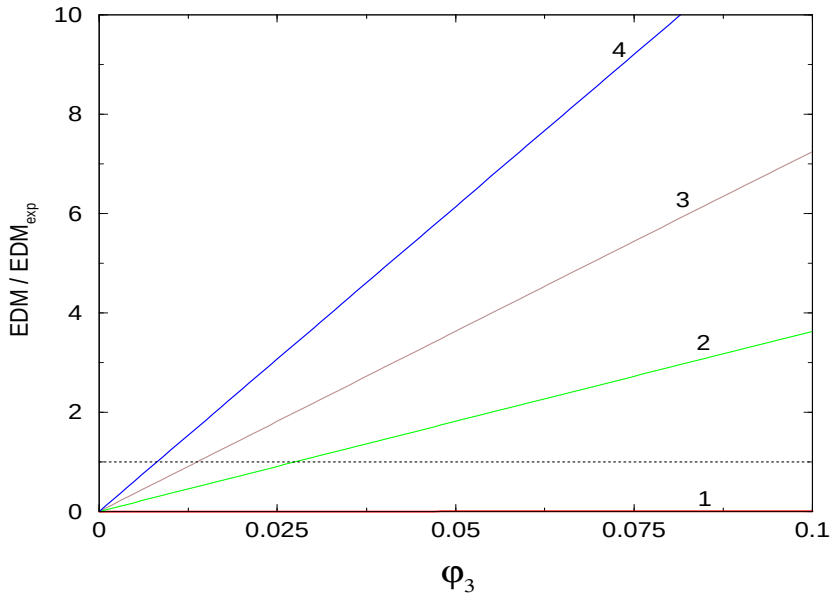


Figure 8: EDMs as a function of the gluino phase ϕ_3. 1 – electron, 2 – neutron (chiral model), 3 – neutron (parton model), 4 – mercury. The experimental limit is given by the horizontal line. Here $\tan\beta = 3$, $m_0 = m_{1/2} = A = 200$ GeV.

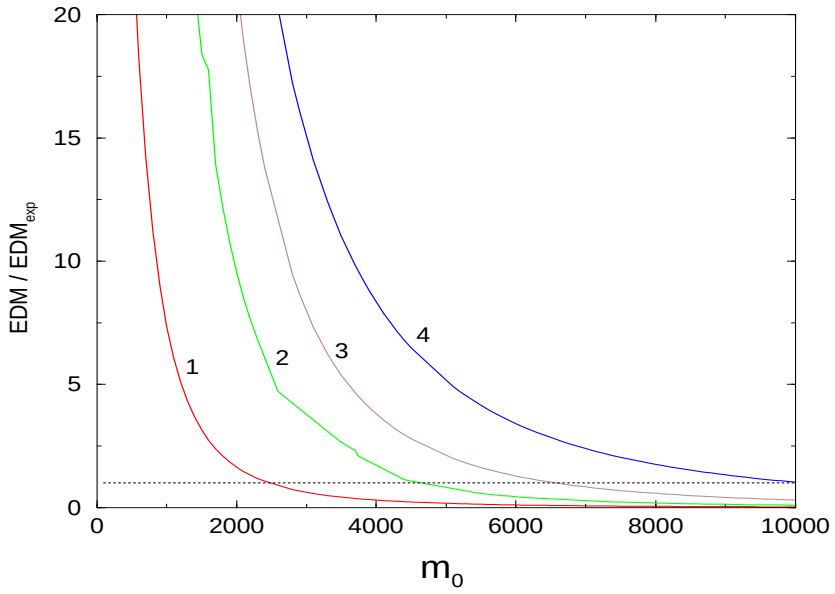


Figure 9: EDMs as a function of the universal mass parameter m_0. 1 – electron, 2 – neutron (chiral model), 3 – neutron (parton model), 4 – mercury. The experimental limit is given by the horizontal line. Here $\tan\beta = 3$, $m_{1/2} = A = 200$ GeV, $\phi_\mu = \phi_A = \pi/2$.

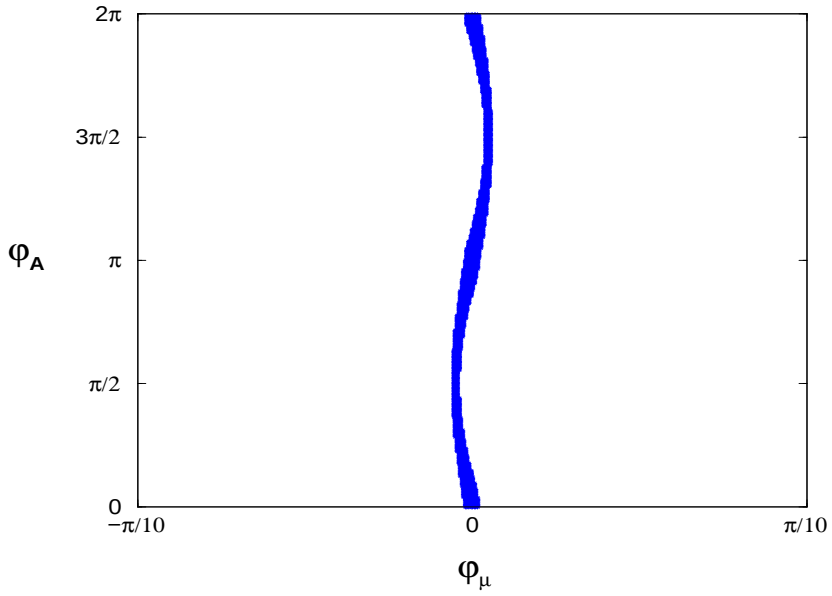


Figure 10: Phases allowed by simultaneous electron, neutron, and mercury EDM cancellations in mSUGRA. The *chiral* quark neutron model is assumed. Here $\tan\beta = 3$, $m_0 = m_{1/2} = 200$ GeV, $A = 40$ GeV.

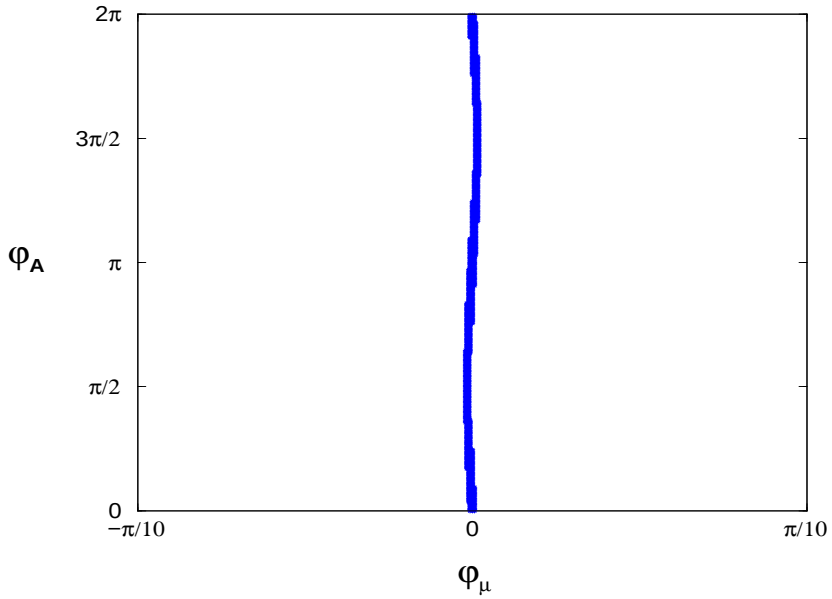


Figure 11: Phases allowed by simultaneous electron, neutron, and mercury EDM cancellations in mSUGRA. The *parton* quark neutron model is assumed. Here $\tan\beta = 3$, $m_0 = m_{1/2} = 200$ GeV, $A = 20$ GeV.

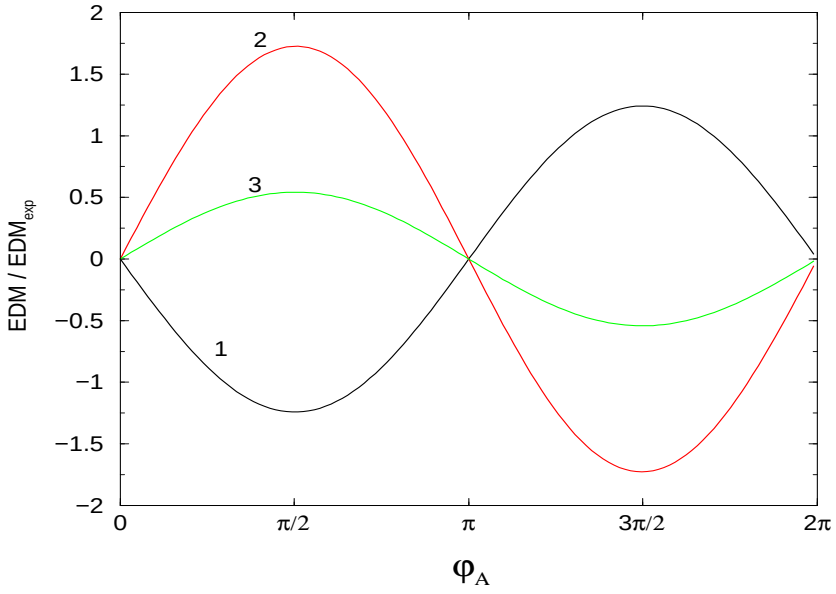


Figure 12: Chargino - neutralino cancellations for the EEDM. 1 – neutralino, 2 – chargino, 3 – total EDM. The SUSY parameters are the same as for Fig.10, which allow for simultaneous electron, neutron, and mercury EDM cancellations.

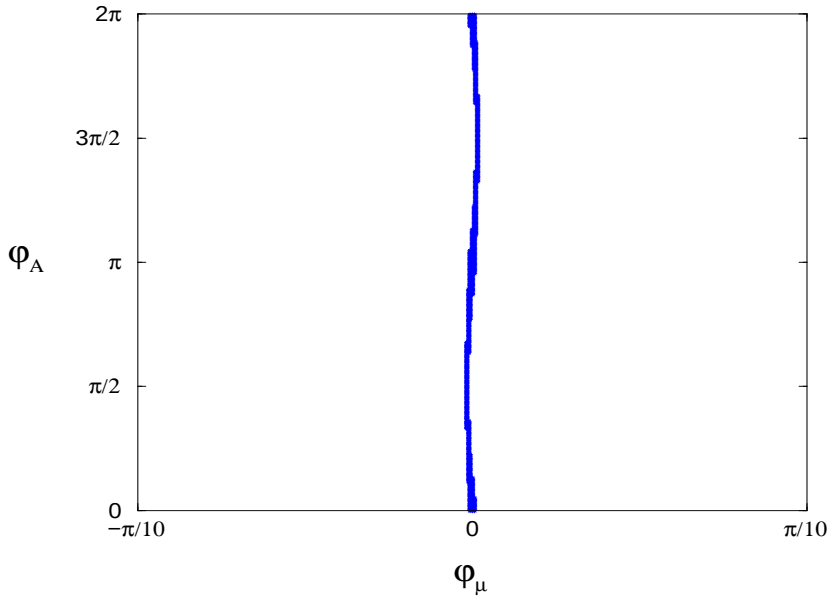


Figure 13: Phases allowed by simultaneous electron, neutron (chiral model), and mercury EDM cancellations in mSUGRA at larger $\tan\beta$. Here $\tan\beta = 10$, $m_0 = m_{1/2} = 200$ GeV, $A = 40$ GeV.

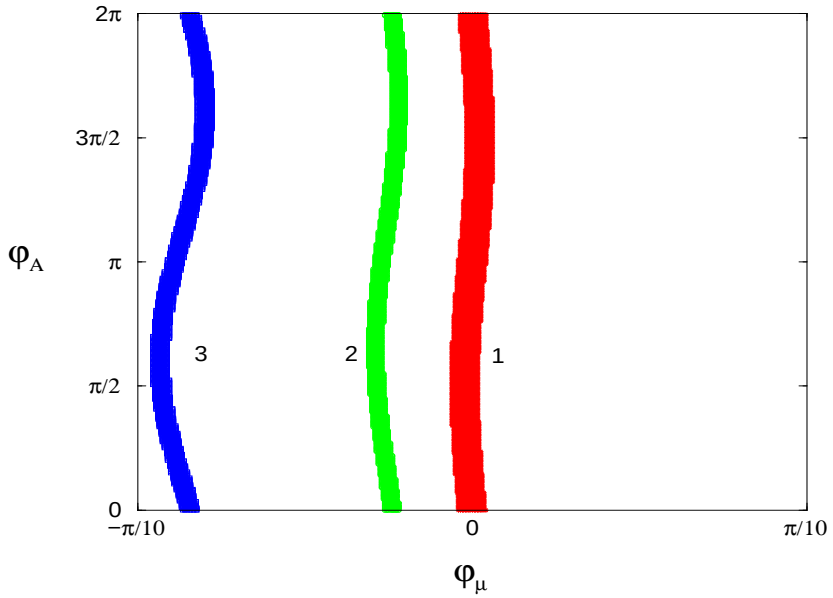


Figure 14: Bands allowed by the electron (1), neutron (2), and mercury (3) EDMs cancellations in the mSUGRA-type model with a nonzero gluino phase. Here $\tan\beta = 3$, $m_0 = m_{1/2} = 200$ GeV, $A = 40$ GeV, $\phi_3 = \pi/10$.

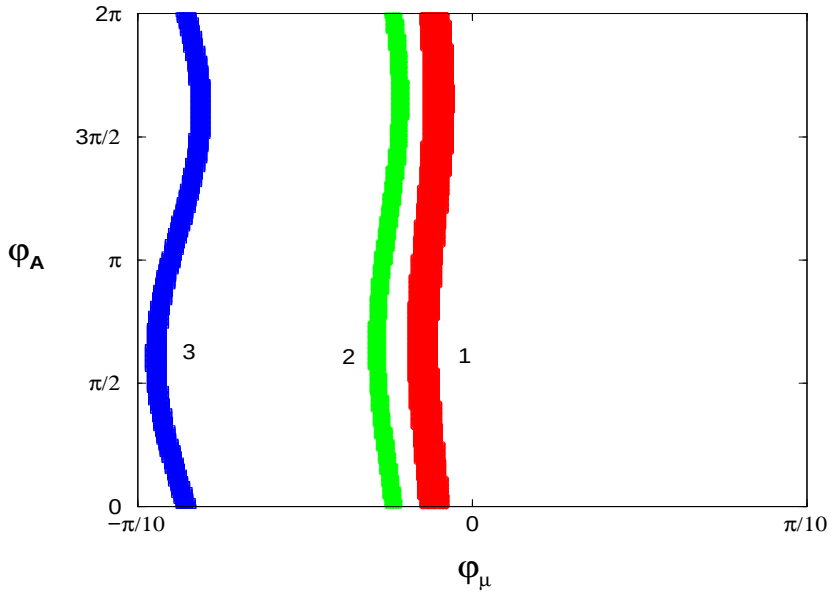


Figure 15: Bands allowed by the electron (1), neutron (2), and mercury (3) EDMs cancellations in the mSUGRA-type model with nonzero gluino and bino phases. Here $\tan\beta = 3$, $m_0 = m_{1/2} = 200$ GeV, $A = 40$ GeV, $\phi_1 = \phi_3 = \pi/10$.

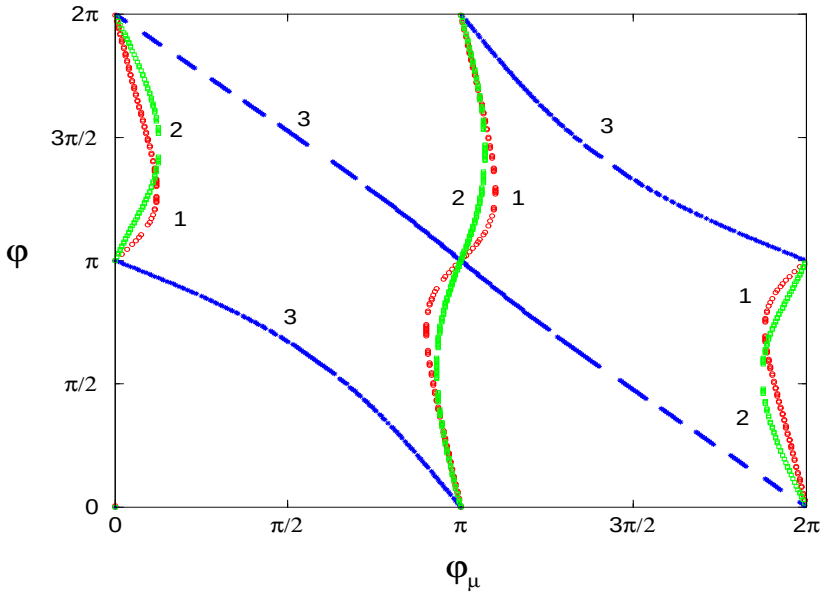


Figure 16: Bands allowed by the electron (1), neutron (2), and mercury (3) EDMs in the D-brane model. Here $\tan\beta = 3$, $m_{3/2} = 150$ GeV, $\Theta_1^2 = \Theta_2^2 = 1/2$, $\cos^2\theta = 2\sin^2\theta = 2/3$, and $M_S \sim 10^{16}$ GeV.

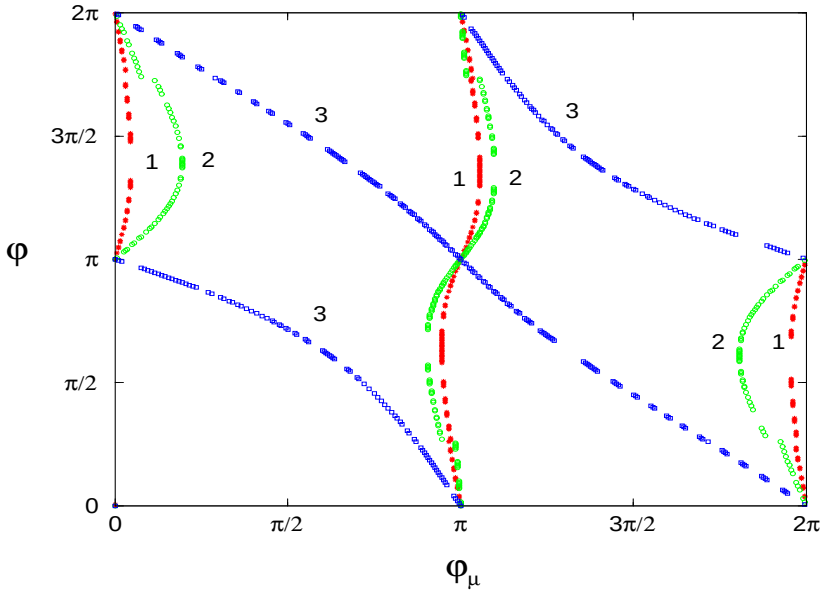


Figure 17: Bands allowed by the electron (1), neutron (2), and mercury (3) EDMs in the D-brane model with an intermediate scale. Here $\tan\beta = 3$, $m_{3/2} = 150$ GeV, $\Theta_1^2 = \Theta_2^2 = 1/2$, $\cos^2\theta = 2\sin^2\theta = 2/3$, and $M_S \sim 10^{12}$ GeV.

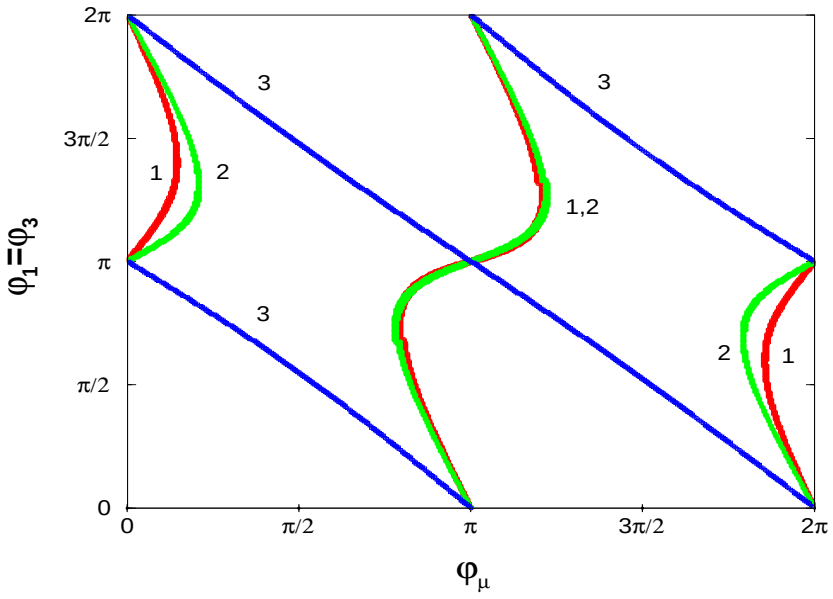


Figure 18: Bands allowed by the electron (1), neutron (2), and mercury (3) EDMs in the model of Ref.[42]. Here $\tan\beta = 2$, $m_{3/2} = 150$ GeV, $\Theta_1 = 0.9$, $\theta = 0.4$.